mater.scichina.com link.springer.com

Published online 14 April 2023 | https://doi.org/10.1007/s40843-022-2397-y
Sci China Mater 2023, 66(5): 1702–1718

Recent application progress and key challenges of biomass-derived carbons in resistive strain/pressure sensor

Lu Wu[1†], Xiaoyu Shi[1†], Pratteek Das[1] and Zhong-Shuai Wu[1,2*]

ABSTRACT **Resistive strain/pressure sensors have attracted intensive attention due to their irreplaceable role in the fields of motor behavior monitoring, human health diagnosis, and human machine interface. Notably, the material and structural design have significant impacts on the performance of resistive strain/pressure sensors. Biomass-derived carbons (BDCs) are considered as popular candidates for realizing the fabrication of resistive strain/pressure sensors because of their excellent properties such as abundant sources, diverse structures, and satisfactory electrical conductivity. This review presents the recent progress of BDCs in the field of resistive strain/pressure sensors and their key challenges. First, the classification methods, evaluation criteria and sensing mechanisms of previously reported resistive strain/pressure sensors are systematically outlined and discussed. Subsequently, the preparation of BDCs with different macrostructures, including one-dimensional (1D), 2D, and 3D structures, and their recent progress in the field of resistive strain/pressure sensors are summarized. Next, the respective advantages of BDCs with different macroscopic structures in the field of resistive strain/pressure sensors are carefully analyzed, and the relationship between different structures and the comprehensive sensing performances of devices is discussed. Finally, the future prospects and major challenges are proposed for BDC-based resistive strain/pressure sensors, and some key future research directions are given.**

Keywords: biomass-derived carbon, resistive strain/pressure sensors, macroscopic structures, wearable electronic devices

INTRODUCTION

With the improvement of living standards, people are becoming more concerned about their health in addition to food and clothing, which has stimulated the rapid development of wearable devices with health signal monitoring capability [1,2]. As a kind of core functional component of wearable devices, strain/pressure sensors have received widespread attention for their simple structure, high accuracy, good stability, and small device size [3–8].

The conventional strain/pressure sensor is mainly composed of a flexible substrate and conductive material, where the conductive material plays important roles in the signal conversion and transmission, determining the sensitivity [9], response time [10], and hysteresis behavior [11] of the sensor. Currently, various functional materials, such as carbon materials [12–14], metal nanomaterials [15,16], and conducting polymers [17,18] have been intensively applied for different types of resistive strain/pressure sensors. Among them, carbon materials have excellent intrinsic properties such as high electrical conductivity, good thermal stability and low toxicity, endowing them with great potential for applications in resistive strain/pressure sensors [19,20]. Moreover, carbon materials can be easily modified by oxidation and grafting to enhance their compatibility with the flexible substrate, which simultaneously holds promise for improving the strain stability and long-term service life of the sensors [21]. Especially, biomass-derived carbon (BDC) exhibits unparalleled and unique advantages over some typical carbon nanomaterials such as carbon nanotubes (CNT) and graphene. For example, BDCs can be obtained from natural materials such as wood [22,23], silk [24], crustacean shellfish [25], and leaves [26,27] through a carbonization process, exhibiting advantages of abundant raw materials [28], diverse structures and ideal sensing performance (Fig. 1), which is extremely attractive to offer the possibility for sustainable development of resistive strain/pressure sensors [29]. Moreover, natural materials are usually macroscopic, suitable for being made into sensors with special morphologies, such as films, fabrics, and fibers, which can offer a perfect shape retention after carbonization and facilitate its combination with flexible substrates [30,31]. For instance, cotton fibers mainly composed of cellulose can be woven into fabrics with controlled thickness and patterns, and the woven structure which can be well maintained after a carbonization process allows ideal connection of carbon networks and contributes to the high electrical conductivity [32]. Table 1 summarizes recently reported representative BDCs for resistive strain/pressure sensors. It is clear from Table 1 that the comprehensive performance of BDC-based resistive strain/pressure sensors is influenced by a variety of factors, including material type, microstructure, and composite strategy. It is generally believed that the structure and composition of the material contribute more to the sensing performance than the device preparation and carbonization process.

Here, we review the latest advances in design and preparation strategies of various BDCs and present their recent application progress in the field of resistive strain/pressure sensors. Firstly, the operating mechanism and the main performance evaluation parameters of resistive strain/pressure sensors are outlined and

[1] State Key Laboratory of Catalysis, Dalian Institute of Chemical Physics, Chinese Academy of Sciences, Dalian 116023, China
[2] Dalian National Laboratory for Clean Energy, Chinese Academy of Sciences, Dalian 116023, China
[†] These authors contributed equally to this work.
[*] Corresponding author (email: wuzs@dicp.ac.cn)

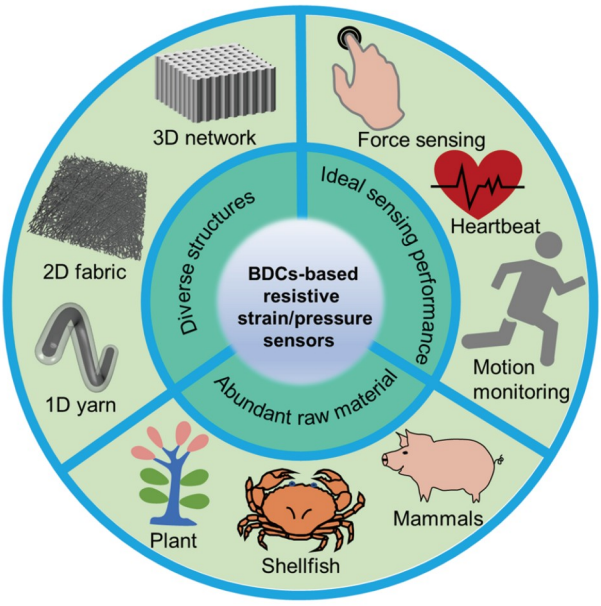

Figure 1 Advantages of BDCs in the field of resistive strain/pressure sensors: abundant raw materials, diverse structures, and ideal sensing performance.

described briefly. Subsequently, the core relationship between the structure of BDCs and sensor performance is discussed and analyzed in detail. Finally, the challenges regarding their application and future directions of BDCs in the field of resistive strain/pressure sensors are briefly proposed. We believe that this review can help readers gain a deeper understanding of BDCs and sensors, and open a window for advancing the sustainable development of resistive strain/pressure sensors with high performance.

SENSING MECHANISM AND PERFORMANCE EVALUATION PARAMETERS

Sensing mechanism

Strain/pressure sensors are mainly composed of a conductive carbon layer and a polymer substrate with good flexibility [33], which can convert the mechanical signals generated by external stimuli into electrical signals [34]. Specifically, the motion of joints and muscles can cause a deformation or pressure stimulation in the sensor in wearable applications, which further leads to changes in the electrical properties of the sensor, making it possible to achieve the goal of detecting human movement and physiological signals. According to the operating mechanism, common strain/pressure sensors are divided into three main types: resistive, capacitive and piezoelectric types (Fig. 2) [5,35,36].

The core operating mechanism of resistive strain/pressure sensors is the change in the conductive network due to external forces [37–40], which can be recorded as resistance changes and smoothly converted into and manipulated as other signals through an external circuit (Fig. 2a, b) [41]. For capacitive strain/pressure sensors, the electrical signal generation mainly relies on the change of capacitance caused by the change of distance or area between the two electrodes, and the invariability of this structure is the biggest drawback of this kind of sensor (Fig. 2a, b) [42]. The key component of piezoelectric sensors is the piezoelectric material that can convert the external force into a voltage electrical signal [43,44]. Unfortunately, the vast majority of piezoelectric sensors are pressure sensors and have difficulty in coping with complex strain behavior (Fig. 2b). Compared with capacitive and piezoelectric sensors, resistive strain/pressure sensors represent unique advantages including simple device structure, ease of preparation, and simple signal reading system, allowing them to become the most popular class of strain/pressure sensors.

Main performance evaluation parameters

The main performance parameters of resistive strain/pressure sensors include sensitivity [59], sensing range [60], response time and fatigue resistance [61,62], which are used to effectively evaluate the real-time performance and reliability of the device detection, having crucial implications for the real-life applications of sensors. Sensitivity is the most important criteria for evaluating the performance of sensors [63]. A high sensitivity signifies that the sensor possesses the ideal ability to capture and

Table 1 Summary of BDCs for resistive strain/pressure sensors

Raw materials	Preparation Strategy	Sensor type	Sensitivity	Sensing range	Cycle life	Ref.
Cotton	800°C, Ar	Pressure	–	0–16 kPa	12,000	[45]
Cotton	800°C, Ar	Pressure	13.89 kPa^{-1}	0–6 kPa	500	[46]
Kapok fiber	800°C, N_2	Pressure	0.44 kPa^{-1}	0–5 kPa	–	[47]
Silk	1050°C, Ar–H_2	Pressure	4.5 kPa^{-1}	0–15 kPa	5000	[48]
Silk	800°C, Ar	Pressure	34.47 kPa^{-1}	0–5 kPa	10,000	[49]
Cotton/graphene	800°C, Ar	Pressure	2.77 kPa^{-1}	0–12 kPa	–	[31]
Cellulose/CNTs	800°C, N_2	Pressure	5.6 kPa^{-1}	0–0.2 kPa	12,000	[50]
Chitosan/cellulose	800°C, Ar	Pressure	27.2 kPa^{-1}	0–18 kPa	30,000	[51]
Cotton	700–900°C, Ar	Strain	GF = 24.1	0–100%	25,000	[52]
Silk	900°C, Ar–H_2	Strain	GF = 173	0–100%	10,000	[53]
Chinese art paper	1060°C, Ar	Strain	GF = 248	0–100%	5000	[54]
Balsa wood	1000°C, Ar	Strain	–	0–20%	5000	[55]
Cotton	900°C, Ar–H_2	Strain	GF = 64	0–140%	2000	[56]
Bamboo	1000°C, N_2	Strain	GF = 30.6	0–60%	1000	[57]
Tissue paper	800°C, N_2	Strain	GF = 10.1	0–5%	10,000	[58]

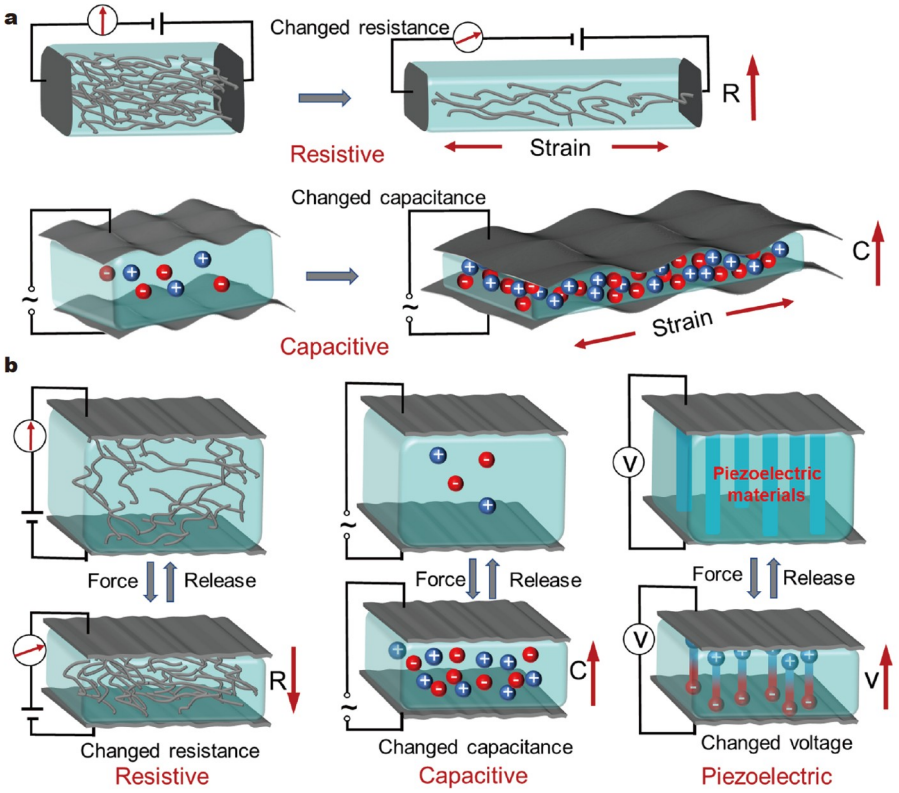

Figure 2 Schematic diagrams of the sensing mechanisms of different strain/pressure sensors: (a) resistive and capacitive strain sensors, (b) resistive, capacitive and piezoelectric pressure sensors.

record small strains or weak pressures [64]. For resistive strain sensors, the sensitivity can be reflected by the rate of resistance change relative to the deformation, also known as gauge factor (GF), which is usually defined according to Equation (1) [65]:

$$\text{GF} = (\Delta R/R_0)/\varepsilon, \quad (1)$$

where R_0 is the initial resistance of the test sample, ΔR is the resistance change of the sample during the tensile deformation, and ε is the deformation of the sample.

For pressure sensors, sensitivity is defined as the change rate of resistance relative to pressure and can be calculated from Equation (2) [66,67]:

$$\text{Pressure sensitivity} = (\Delta R/R_0)/P, \quad (2)$$

where R_0 and ΔR are the initial resistance of the test sample and the resistance change during compression, respectively, and P is the applied pressure.

The sensing range is the maximum tensile deformation or compressive force value at which the sensor could maintain stable and repeatable sensing behavior. A wide sensing range ensures outstanding structural integrity of the sensor under large deformations [68,69]. When sensors are used for body movement detection, high sensitivity facilitates the sensing of subtle vibration signals, such as pulse, breath, and speech, while large range of joint movements, such as bending of finger or knee, requires a wide sensing range to avoid damage to the sensor from limb movements [70]. For pressure sensors, the sensing range usually refers to the ultimate pressure range within which the material can maintain linear sensing behavior. For strain sensors, the ratio of the maximum deformation of sensor to its original length is used to evaluate the sensing range, expressed by Equation (3) [71]:

$$\text{Stain range} = \Delta L/L_0, \quad (3)$$

where L_0 and ΔL are the original length and the maximum deformation variable, respectively.

Response time is the time taken for the resistance to change when the sensor is deformed by an external force, and hysteresis is the difference in the value of resistance change of the sensor during the load-unload cycle with the same strain [72,73], reflecting the ability to monitor the strain or pressure in real time. Shorter response time and weaker hysteresis behavior of the sensor represent better real-time performance of the device [74]. For repetitive strains or pressures within very short time-intervals, such as pulse or heartbeat, the short response time can guarantee that each strain or pressure is recorded accurately and timely, which is important for the sensing of high-frequency and real-life pressure stimuli. During repeated testing and operation process, the conductive network in strain/pressure sensors would undergo unavoidable creep or fatigue breakage behavior, resulting in some defects in the conductive network and reduction of the sensor accuracy. Therefore, the ideal resistive strain/pressure sensors are required to have excellent resistance to mechanical fatigue and durability to maintain stable output of the electrical signal during long-term load-unload repetitive cycles. The fatigue resistance can be analyzed by the degree of overlap of the strain-recovery cycle hysteresis curves [75]. A high degree of overlapping means that the sensor can recover smoothly to its original state after experiencing strain and signifies excellent fatigue resistance [76,77].

BDCs FOR STRAIN/PRESSURE SENSORS

Biomass materials, including plant-based and animal-based

biomass, are distributed in almost every corner of the earth and make up a colorful world with incredible living organisms [78,79]. The composition and structure of biomass materials are complex and usually contain C, H, O and N elements, which constitute the basic components of living organisms such as carbohydrates and protein [80,81]. Fig. 3 depicts the composition and molecular structure of some important biomass materials. Representatively, plants are the most common precursors for the preparation of BDCs, due to their high cellulose (about 50 wt%) and lignin (20–40 wt%) contents [82]. Cellulose, as the most abundant natural polymer on earth, is a linear macromolecule composed of β-(1,4)-linked *D*-glucose units, and the high C content and the tightly arranged carbon skeleton are very favorable for the carbonization process and the high conversion rate of derived carbon (Fig. 3a) [83,84]. Lignin possesses the second highest content inferior only to cellulose in plants and is the most natural aromatic chemical on earth [85]. Lignin is a phenolic polymer with a high aromatic ring content prepared by the dehydrogenation polymerization of aromatic alcohol precursors (sinapyl alcohol, coniferyl alcohol and *p*-coumaryl alcohol) [86], which can facilitate the preparation of structurally dense derived carbon (Fig. 3a) [87]. Animal-based biomass materials can be divided into two main types: (1) chitin and chitosan linked by ether bonds; and (2) protein aggregates linked by peptide bonds. As an important nitrogenous biopolysaccharide, chitin is widely distributed in nature and the basic substance forming the exoskeleton of crustaceans, insects and other organisms (Fig. 3b) [88,89]. Different extraction sources affect the internal crystal structure of chitin and consequently alter their thermal stability and carbonization processes. In general, the initial thermal decomposition temperature of chitin is close to 280°C, which is higher than that of cellulose and not suitable for the carbonization process by the hydrothermal strategy [90–92]. Therefore, most of chitin-derived carbons are prepared by pyrolysis in an inert gas atmosphere. In contrast, chitosan, a derivative of chitin produced by a deacetylation process, has a lower initial pyrolysis temperature and desirable solubility [93], which offers its convenience for the preparation of derived carbons with specific macroscopic shapes through an integrated dissolution-gel-carbonation strategy. Besides, silk, an aggregate of structural proteins, is another representative animal-based biomass in which proteins form β-sheet microcrystals that are easily transformed into sp^2 hybridized carbon structures under heat treatment (Fig. 3c), making it an ideal candidate for the production of derived carbons. Further, the fibrous silk can be woven into two-dimensional (2D) fabrics, offering the possibility for large-scale preparation of BDCs with regular morphology [94,95]. Notably, the fabric-derived carbons prepared on a large scale often exhibit good flexibility, allowing for easy integration with clothing for wearable devices. In this section, we

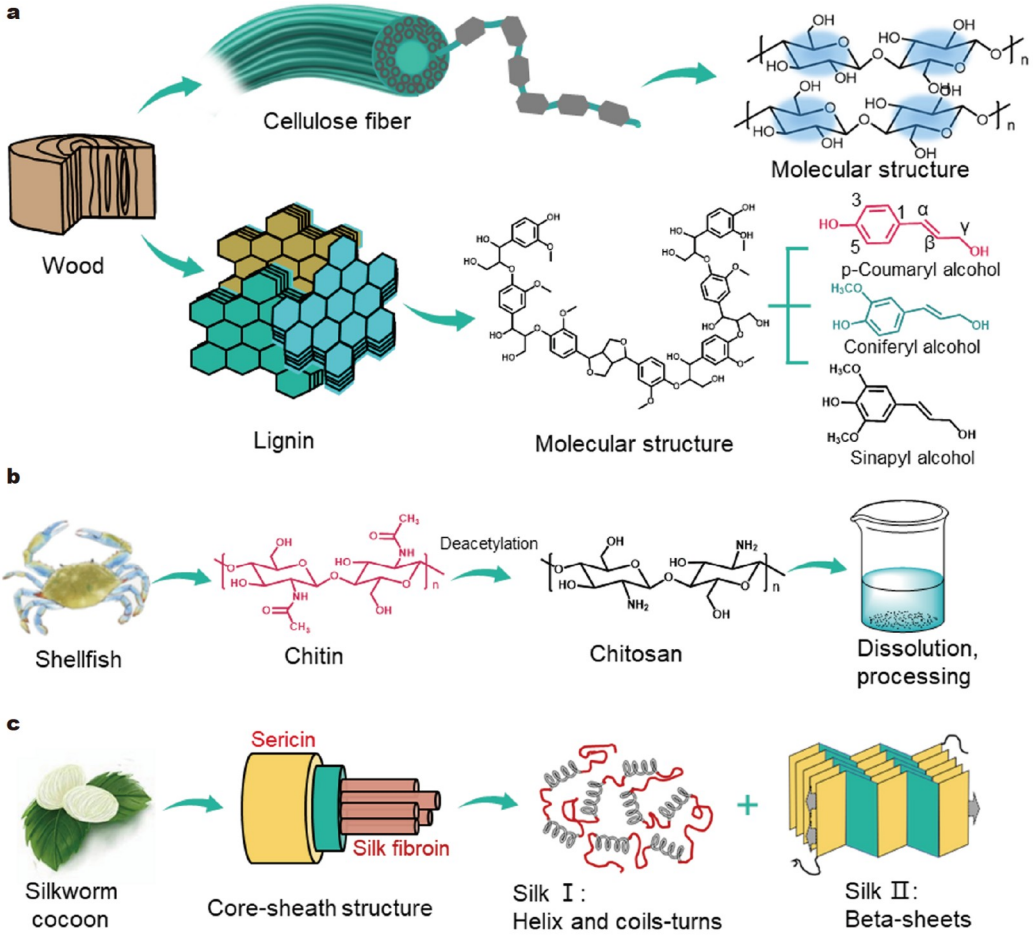

Figure 3 Representative biomass materials and their molecular structures. (a) Molecular structure of cellulose and lignin. (b) Molecular structure of chitin and soluble chitosan. (c) Core-sheath structure of silk and the structure of silk protein.

summarize the recent research progress by focusing on BDCs with different macroscopic structures, including 1D, 2D, and 3D structures, in the applications of strain/pressure sensors, and discuss the difficulties and existing challenges.

1D strain/pressure sensor

The 1D biomass materials, mainly formed by the aggregation of macromolecules through intermolecular forces, are widely distributed in nature, and their main existing forms include silk, cotton fibers and animal hair. The molecular backbone of these natural fibers contains a large amount of carbon, which allows them to be converted into conductive carbon materials through an anaerobic carbonization process. Further, these natural fibers can be spun into continuous and long 1D yarns, providing great convenience for their actual applications. Typically, current 1D sensors manufactured using carbon materials include CNT yarns [96,97], and graphene yarns [98,99], but the macroscopic powder state of these carbon materials greatly increases the difficulty of processing them into yarns. Besides, the yarn preparation process usually involves the polymer incorporation. For example, even with the help of elastomeric polyurethane, CNT yarn preparation must undergo a complex process of dissolution-spinning-drying (Fig. 4a) [100]. In contrast, natural fibers have a large aspect ratio and good processability and can be easily spun into yarns, which ensures the integrity of 1D carbonized yarns. Moreover, natural fiber can be formed smoothly into helical or sheath-core structures by combining with other materials, which is helpful to take full advantages of the driven carbon materials and ensures high GF values and wide strain sensing range of the sensors [101,102]. In this regard, Yan *et al.* [103] developed a series of 1D yarn strain sensors with adjustable sensing range and GF value by carbonizing a spiral composite of cotton or silk yarn and carbon nanofiber (Fig. 4b). The carbonized composite yarns showed a sheath-core structure with a good spiral morphology (Fig. 4c). The GF and sensing range of the carbonized yarn strain sensors encapsulated by Ecoflex rubber could be readily controlled by adjusting the combination of carbonized precursors, facilitating the customizable construction of sensors towards different situations. When choosing silk as the core and carbon nanofiber yarn as the sheath, the resulting sensor (Sensor 1) showed an extremely high GF value of over 300 (Fig. 4d) and a high linear sensing behavior of R^2 = 0.97 within 5% working deformation (Fig. 4e). In addition, this 1D strain sensor had a short response time of only 0.4 s and could withstand over 1000 strain cycles, manifesting excellent instantaneous response ability and long service life. Moreover, the 1D sensor prepared from a combination of silk and cotton fibers (Sensor 3) displayed less GF (2.77), but exhibited an extended sensing range of more than 120%, indicative of favorable customization (Fig. 4f). Notably, this 1D yarn sensor (Sensor 3) could capture the subtle

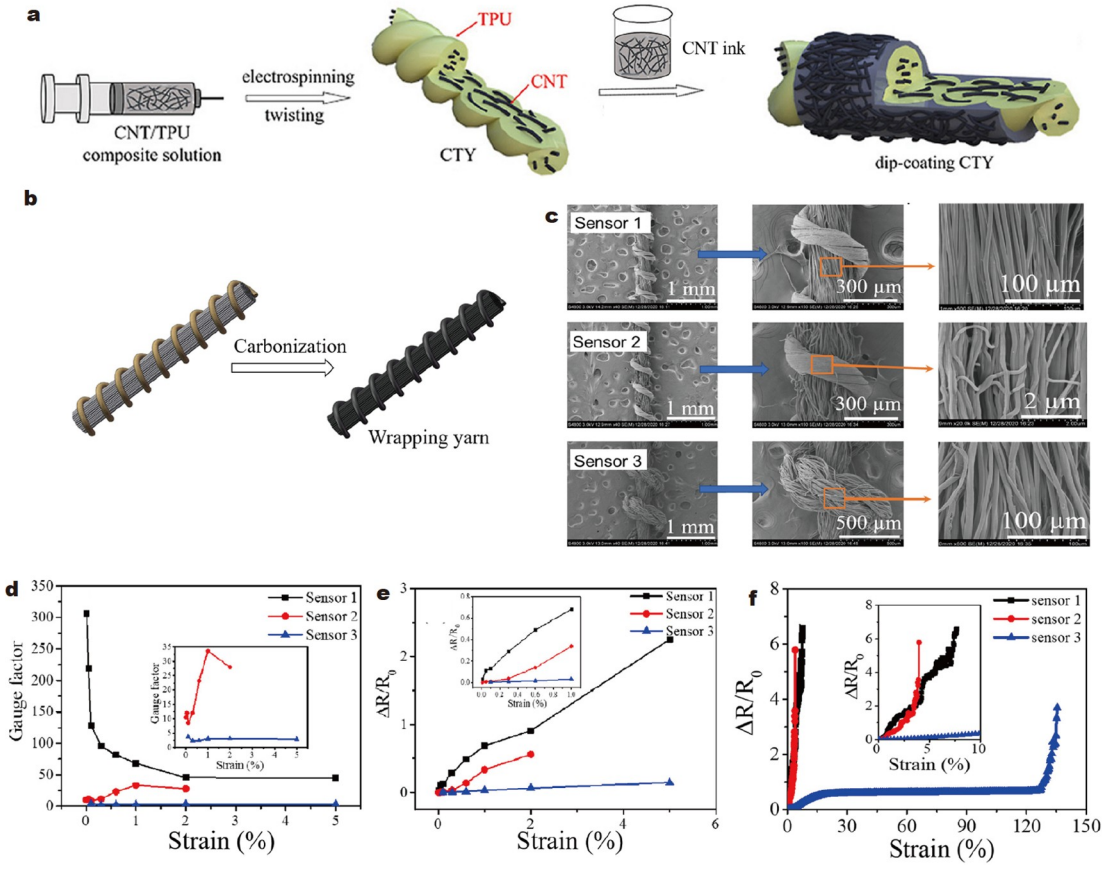

Figure 4 Structure and performance of 1D strain sensors. (a) Preparation process of CNT/polyurethane composite yarn. Reprinted with permission from Ref. [100]. Copyright 2022, Elsevier. (b) Schematic diagram of the structure of the composite yarn. (c) Scanning electron microscopy (SEM) images of different carbonized yarns: silk-carbon nanofiber yarn composite (Sensor 1), cotton fiber-carbon nanofiber yarn composite (Sensor 2), and silk-cotton fiber composite (Sensor 3). (d) GF values for different 1D yarn sensors. (e) Change of sensor resistance at the initial stage of stretching. (f) Relationship between deformation variables and resistance change of different 1D yarn sensors. Reprinted with permission from Ref. [103]. Copyright 2020, Elsevier.

vibrations generated by pulse and give timely and repetitive electrical signal feedback. Unfortunately, there are few studies on 1D BDC-based resistive strain/pressure sensors. Therefore, it is urgently required to explore BDC-based 1D structural resistive strain/pressure sensors with large strain sensing range and high sensitivity.

2D strain/pressure sensors

The 1D strain sensor accurately captures the strain in the direction of the fiber axis and gives timely and reliable electrical signal feedback. Whereas, the human skin exhibits a nearly 2D flat structure, and the strain on the skin during movement is complex and has no fixed direction in general, which raises higher demands on structure of the sensor (Fig. 5a). In this case, plentiful natural biomass fibers, including cotton fibers, chitosan fibers, and silk, can be easily processed into 2D fabrics [104,105], which then ensures the fabrication of derived carbon-based devices with customizable shapes (Fig. 5b). Besides, compared with 1D sensors, a 2D structure can fit more closely with human skin, beneficial to effectively detect the strain stimuli from different directions and ensure the perfect electrical signal output.

Wang *et al.* [106] prepared highly sensitive, stretchable and wearable 2D sensors by programmed carbonization of silk (Fig. 6a). The resulting silk-derived carbon showed an intact morphology (Fig. 6b), continuous network with good electrical conductivity, and ability of bending up to 180°. After polydimethylsiloxane (PDMS) encapsulation, the strain sensing range of the silk-derived carbon-based sensor exceeded 500%, benefiting from the complete and continuous conductive network of the carbonized silk. Furthermore, within the strain range of 250%, the sensor exhibited satisfactory linear sensing behavior with a GF of 9.6, while the GF rapidly increased to a higher value of 37.5 in the strain from 250% to 500%, owing to the rapid disruption of the conductive network under large deformation. Notably, based on the sensor's wide tolerable strain, the silk-derived carbon-based sensor could still maintain

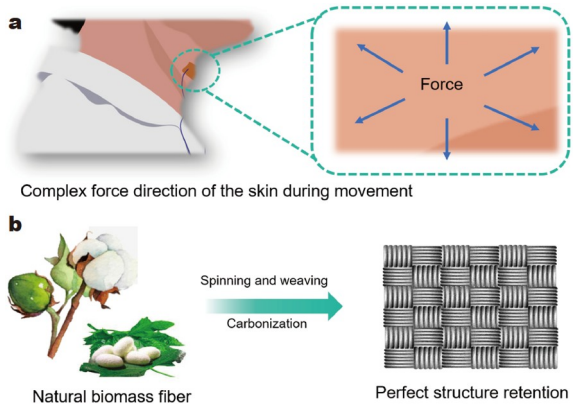

Figure 5 The unique properties of human skin and biomass fibers. (a) Complex external force direction on the skin when limb movements occur. (b) Perfect retention of the fabric microstructure after carbonization.

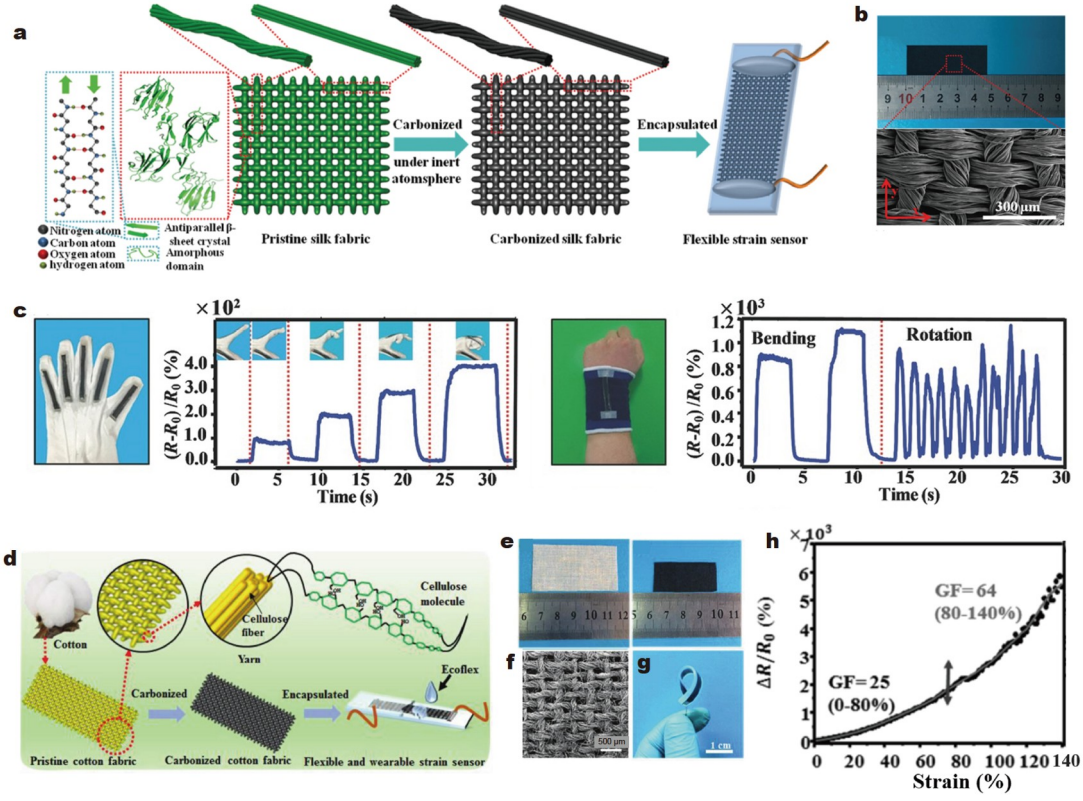

Figure 6 Preparation and performance of carbon-based strain sensors derived from 2D biomass fiber-based fabric. (a) Preparation schematic of silk-derived carbon-based 2D strain sensors. (b) Digital photograph and SEM image of the silk after carbonization. (c) Integration of silk-derived carbon-based strain sensors and monitoring behavior of joint flexion movements. Reprinted with permission from Ref. [106]. Copyright 2016, Wiley. (d) Structure of cotton fabric and the preparation process of cotton fabric-derived carbon-based 2D sensors. (e) Digital photographs of cotton fabrics before and after carbonization. (f) SEM image of the 2D cotton fabric after carbonization. (g) Excellent flexibility of cotton fabric-derived carbon-based 2D sensors. (h) Comprehensive sensing performance of cotton fabric-derived carbon-based 2D sensors. Reprinted with permission from Ref. [56]. Copyright 2017, Wiley.

almost the same electrical signal change as the initial value after 6000 cycles of large 100% strain, implying a long service life and excellent fatigue resistance property. With its surprising flexibility and complete 2D structure, the silk-derived carbon-based sensor could be integrated into a glove or wrist guard to detect finger-wrist bending movements and even pulse in real time, exemplifying great potential for wearable health-monitoring applications (Fig. 6c). In addition, cotton and flax also display complete fiber structure, which allows them as common raw materials to be transformed into 2D derived carbon fabrics [107]. For instance, Zhang *et al.* [56] prepared a cotton fabric-based strain sensor by carbonization in an inert gas (Fig. 6d). After carbonization, the absence of a large number of elements led to a significant volume contraction of the cotton fabric, accompanied with changes in surface area and mass of more than 49% and 80%, respectively (Fig. 6e). Nevertheless, the carbonized cotton fabric still demonstrated a complete crisscross pattern and continuous fiber network (Fig. 6f), signifying superior flexibility of the sensor (Fig. 6g). This sensor could tolerate 140% of the strain and maintain a stable and high GF value of 25 in the 0–80% strain range (Fig. 6h). Fascinatingly, the sensor could even sense an ultralow deformation of 0.02%, indicative of an extraordinary ability to capture subtle body movements and monitor the heartbeat during different states of motion. More importantly, the simple carbonization process and the short carbonization time of cotton fabrics hold promise for low-cost large-scale preparation of strain sensors.

Paper is another major aggregate of cellulose that has played an irreplaceable role in the development of human civilization for thousands of years [108]. The same molecular structure interprets that the paper can be carbonized as perfectly as cotton fiber fabric to form paper-derived carbons for sensor applications. As a typical example, Chen *et al.* [58] converted commercial tissue paper into a 2D conductive derived carbon network by an easily manipulated carbonization process under N_2 atmosphere, and further prepared strain sensors (Fig. 7a, b). The GF value in the orientation direction could reach 10, which was much higher than the GF value of 0.14 in the non-orientation direction. The anisotropic sensing behavior could also be reflected in the human motion detection process, where the sensor offered different intensity of resistive signal changes to the deformation caused by the human wrist motion in orientation and non-orientation directions. This phenomenon can be explained by the fact that strain stimulation along the orientation direction brings more severe damage to the conductive network, while the non-orientation direction is insensitive to strain (Fig. 7c). More importantly, the integrated tissue paper-derived carbon (TPDC)-based strain sensors could be connected to a robotic arm *via* a microcontroller, enabling it to be motion controlled (Fig. 7d). Although the TPDC-based strain sensors exhibited high strain sensitivity, the inherent anisotropy of the carbonized tissue fibers led to large variations in GF values, which was not conducive to accurately reflecting the strain in different directions. To address this issue, Xia *et al.* [54] chose traditional Chinese Xuan paper as the raw material, transformed it into derived carbon through a simple heat treatment method and constructed strain sensors from it (Fig. 7e). The fiber length of Xuan paper made from *pteroceltis tatarinowii* maxim bark and long-stalked straw fibers could reach 2000 μm, which was favorable for the formation of long-range conductive networks and the improvement of sensing range after carbonization. Besides, the cellulose fibers in Xuan paper formed a disordered network through random overlap (Fig. 7f), and the resulting isotropic structure allowed for perfect sensing of forces from all directions (Fig. 7g). The sensing analysis results showed that the Xuan paper-derived carbon-based sensor exhibited surprisingly linear sensing behavior and stable high GF value of 68 within a large strain sensing range of 0–100%, indicating that the conductive network was broken in an orderly manner during tensile strain. Impressively, this sensor could detect even minute deformations down to 0.01% and quickly yield reproducible electrical signal feedback results, implying a surprising strain sensitivity. This phenomenon was attributed to the extremely dense overlapped network of Xuan paper, which could be destroyed by a very small strain and then lead to a change in resistance. Furthermore, the Xuan paper-derived carbon-based sensor could sense the tensile strain in time and send the same value of resistance change as the initial state even after more than 5000 strain cycles (10%), demonstrative of excellent structure stability and long service life.

More importantly, the 2D planar structure of fabric or paper is conducive to the capture of balanced pressure stimuli, making facile preparation of multifunctional strain/pressure sensors possible. For instance, Xu's group [109] assembled paper-based cross-finger pressure sensors by using carbonized crepe paper and flexible printing paper as conductive network and flexible substrates, respectively (Fig. 8a). The carbonized crepe paper exhibited excellent electrical conductivity and the unique wave-like microstructure, which endowed the sensor with superior pressure sensitivity. This sensor could capture a tiny pressure of about 50 Pa and visibly sense the pulse state before and after the movement and then give the corresponding recognizable electrical signals. What is more, the vibrations caused by playing music, pressure generated by water droplets, and even airflow led by breathing could be recorded by the crepe paper-derived carbon-based sensor. Compared with counterparts based on ordinary printed paper, the crepe paper-derived carbon-based sensor generated greater current changes at the same applied pressure, further demonstrating excellent pressure sensitivity. This result is attributed to the structural differences between crepe paper and printed paper, in which crepe paper displays a porous internal structure and wavy morphology, while printed paper exhibits a dense and flat structure (Fig. 8b, c). Further, the integrated pressure sensor array could monitor the dynamic changes of pressure distribution in real time (Fig. 8d), suggesting significant application prospects in various fields such as human-machine interface and intelligent robot skin.

Notably, the hybridization or composite with other micro- or nano-materials can improve the roughness of the derived carbon surface and amplify the local pressure, which is beneficial for improving the pressure sensitivity. Inspired by the unique structure of sunflower faceplate, Lu *et al.* [48] grew vertically aligned MoS_2 on the surface of carbonized silk and used it as a sensing material for pressure sensors (Fig. 8e). The maximum pressure sensitivity of the carbonized silk/MoS_2 composite reached 11.6 kPa^{-1}, which was a 680% improvement compared with the pure carbonized silk (Fig. 8f). The sensor fixed to the neck of a volunteer could distinguish different sounds from the speaker and obtain easily discernible characteristic electrical signals separately (Fig. 8g).

Besides, MXene, as a novel 2D material with unique physicochemical properties, has often been employed in the fields of

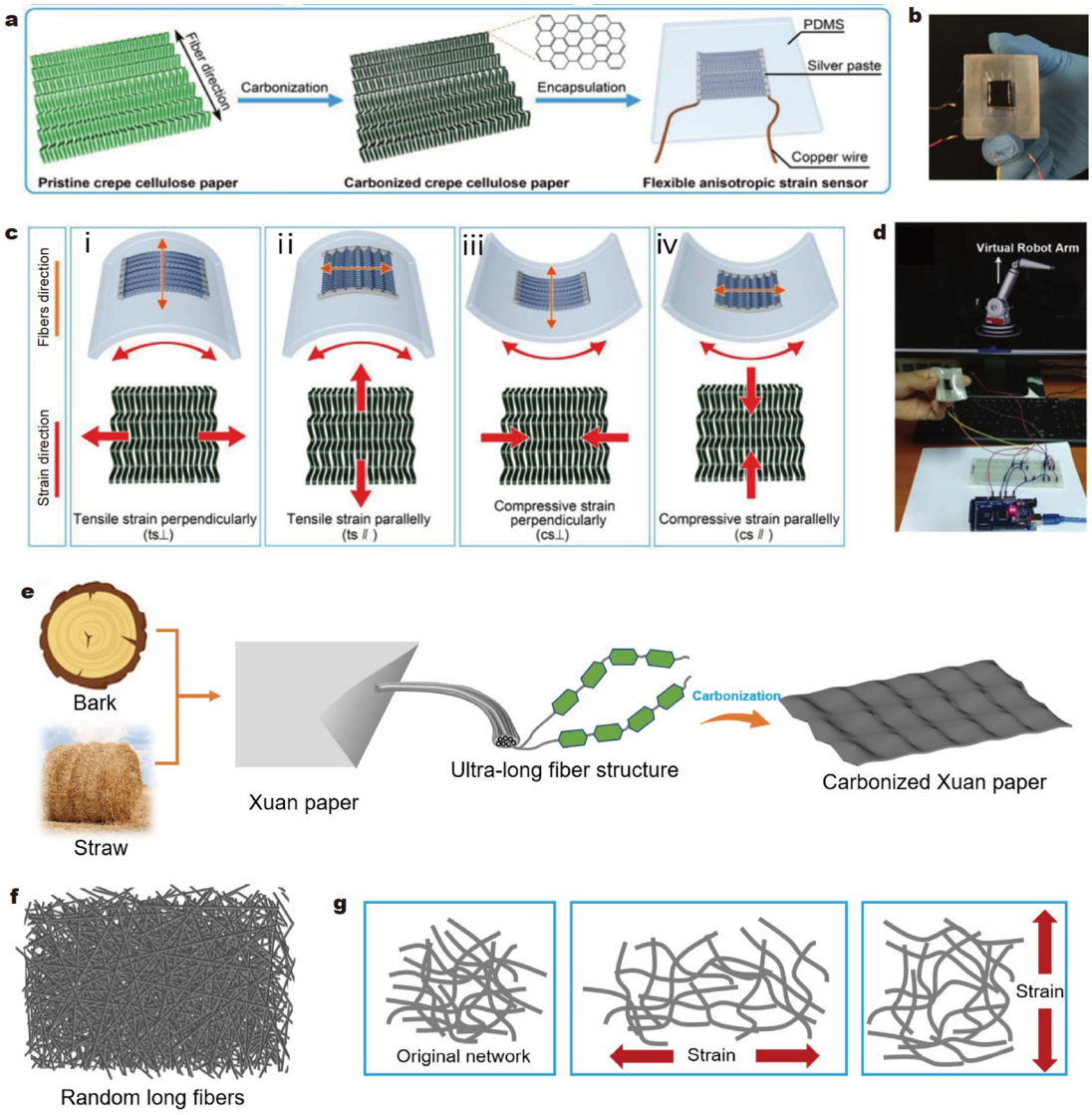

Figure 7 Applications of 2D paper-derived carbons in the field of resistive strain sensors. (a) Schematic diagram of the preparation strategy for TPDC-based strain sensors. (b) Digital photograph of a PDMS-encapsulated TPDC-based strain sensor. (c) Changes in the conductive network of TPDC-based strain sensors when strain occurs in different directions. (d) Digital photograph of the integrated TPDC-based strain sensor and the TPDC-based strain sensor connected to a robot arm. Reprinted with permission from Ref. [58]. Copyright, 2018 Wiley. (e) The carbonization process of Xuan paper and the preparation process of strain sensors. (f) Random long fibers of carbonized Xuan paper. (g) Effect of stress in different directions on the conductive network of carbonized Xuan paper.

sensors, multifunctional composites, etc. [110–112]. For instance, Zheng *et al.* [113] prepared a carbon material derived from a MXene/cotton fabric composite by designing a simple soaking strategy, and then completed the construction of the pressure sensor by sandwiching it between the PDMS film and interdigital electrode. The large number of active groups such as hydroxyl groups on the surface of cotton fibers enabled MXene to be stably anchored on the surface of the fabric, achieving the efficient construction of a highly conductive network. Due to the unique conductive network, this MXene/cotton fabric-derived carbon-based sensor showed a wide sensing range of 0–160 kPa, a fast response time of 50 ms and a high pressure sensitivity of 5.30 kPa^{-1}. Moreover, these excellent properties even permitted it to monitor the limb tremors in early Parkinsonism, implying its potential for applications in the field of health assessment.

In addition to fabric and paper, electrospun fiber membranes are also a class of important 2D macroscopic materials. Uniquely, the membrane morphology and thickness can be accurately controlled by adjusting the spinning time, voltage, and spinning fluid concentration, which contributes to the improvement in device size and transmittance of sensors [114–116]. Typically, Wang *et al.* [49] converted the dissolved silk protein into transparent membranes by electrostatic spinning, and subsequently realized the preparation of transparent conductive silk-derived carbon films by anaerobic carbonization technique (Fig. 8h). In this case, an ultrathin silk membrane of 2 μm was achieved by varying the electrospinning time, which resulted in a high transmittance of up to 80% in the carbonized silk membrane (Fig. 8i) and offered the sensor an ultra-high pressure sensitivity of over 34.47 kPa^{-1} and a surprisingly low detection limit of 0.8 Pa. Besides, the electrospun silk membrane-derived carbon-based strain sensor exhibited an extremely

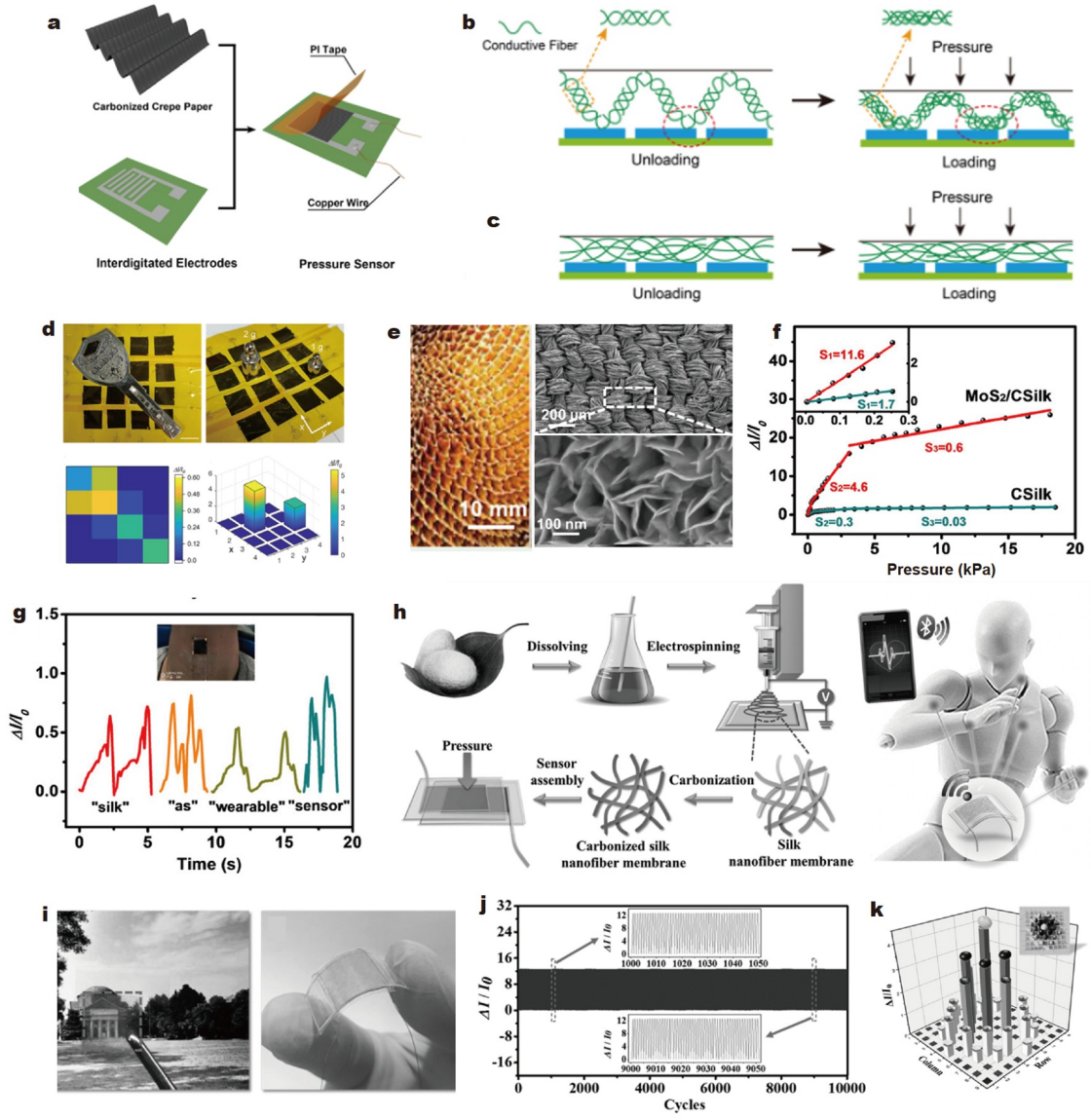

Figure 8 Contribution of 2D BDCs with a unique structure to resistive strain/pressure sensors. (a) Preparation of crepe paper-derived carbon-based sensors. (b) Microstructural changes of crepe paper-derived carbon-based sensors under loading. (c) Microstructural changes of printed paper-derived carbon-based sensors under loading. (d) Crepe paper-derived carbon-based sensors for the detection of spatial pressure distribution. Scale bar: 1 cm. Reprinted with permission from Ref. [109]. Copyright 2018, American Chemical Society. (e) Photograph of sunflower and SEM images of carbonized silk/MoS_2. (f) Pressure sensitivity of carbonized silk/MoS_2 and pure carbonized silk pressure sensors in the pressure range of 0–18.5 kPa. (g) Sensing behavior of carbonized silk/MoS_2 sensors for different pronunciations. Reprinted with permission from Ref. [48]. Copyright 2020, American Chemical Society. (h) Strategy for the preparation of silk protein membrane-derived carbon-based transparent sensors. (i) Transparency and flexibility of silk protein membrane-derived carbon-based sensors. (j) Changes in electrical signals of silk membrane-derived carbon-based sensors during 10,000 pressure-release cycles. (k) Capture of small pressure distributions by silk membrane-derived carbon-based sensor arrays (9 × 9). Reprinted with permission from Ref. [49]. Copyright 2017, Wiley.

short response time of 16.7 ms and a stable repetitive sensing behavior over more than 10,000 cycles (Fig. 8j), indicating superb instantaneous sensing performance and satisfactory cycling stability. In addition to the effective detection of pulse, pressure changes during activities such as fruit picking could also be recorded by the electrospun membrane-derived carbon-based strain sensor, proving its ability to assist daily life of people fitted with prostheses. Moreover, the integrated sensor matrix (9 × 9) could detect the pressure changes brought by small objects such as red beans and rice, and reflect the corresponding pressure distribution (Fig. 8k). The 2D structured sensor achieves simultaneous sensing of pressure and tensile strain, maximizing the flexibility of the sensor and foreshadowing its important future applications in smart clothing, sports detection, and health monitoring.

3D strain/pressure sensors

Some biomass materials in nature usually form macroscopic 3D aggregates, the most representative example of which is wood. Wood, mainly composed of cellulose, hemicellulose, and lignin, is one of the most abundant natural carbon sources and has a unique pore structure (Fig. 9) [22,117], which thereby has emerged as an important precursor for the production of 3D porous carbon materials [22,55,118]. Besides, the selective

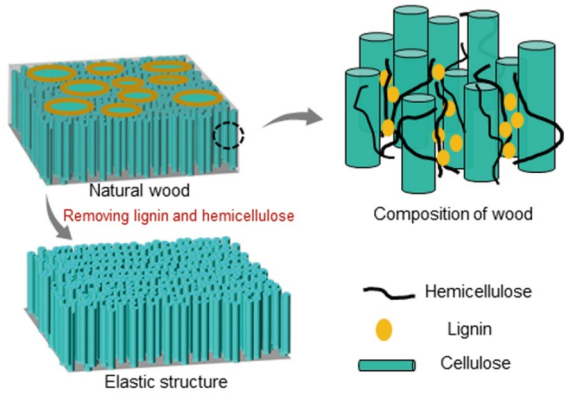

Figure 9 Composition of wood and preparation of elastic wood sponge.

removal of lignin could convert the wood into an elastic aerogel with porous structure, which creates the prerequisite for the preparation of pressure sensors (Fig. 9) [119,120].

For example, Hu's group [121] removed the lignin from wood with the help of sodium sulfite and sodium hydroxide and obtained wood aerogels. On this basis, they further refined the experimental strategy by using chemical reagents including sodium sulfite, sodium hydroxide and H_2O_2 for continuous treatment of virgin wood for achieving complete removal of hemicellulose and lignin and realizing the preparation of wood sponges with an oriented pore structure (Fig. 10a) [122]. Compared with natural wood, the treated wood samples exhibited an ideal arching stacked lamellar structure (Fig. 10b). Moreover, this structure can be perfectly retained even after carbonization, obviously distinguished from the microstructure of the directly carbonized wood. Moreover, carbonized wood sponge could resist over 10,000 compression-release cycles at 50% constant strain without any permanent deformation, signifying outstanding mechanical fatigue resistance. This is because the arching stacked lamellar structure of the carbonized wood sponge weakened the stress concentration compared with the directly carbonized wood, enhancing the material's resistance to compression (Fig. 10c). Further, the carbonized wood sponge could be assembled to a pressure sensor by sandwiching it between two pieces of copper (Fig. 10d). With increasing compressional deformation, the conductivity of the sensor showed a dramatic increase from 0.04 to 1.66 S m^{-1} (Fig. 10e). When the sensor was attached to the model's finger, the generated current increased significantly with the bending of the finger, implying the ability to detect human motion. Unfortu-

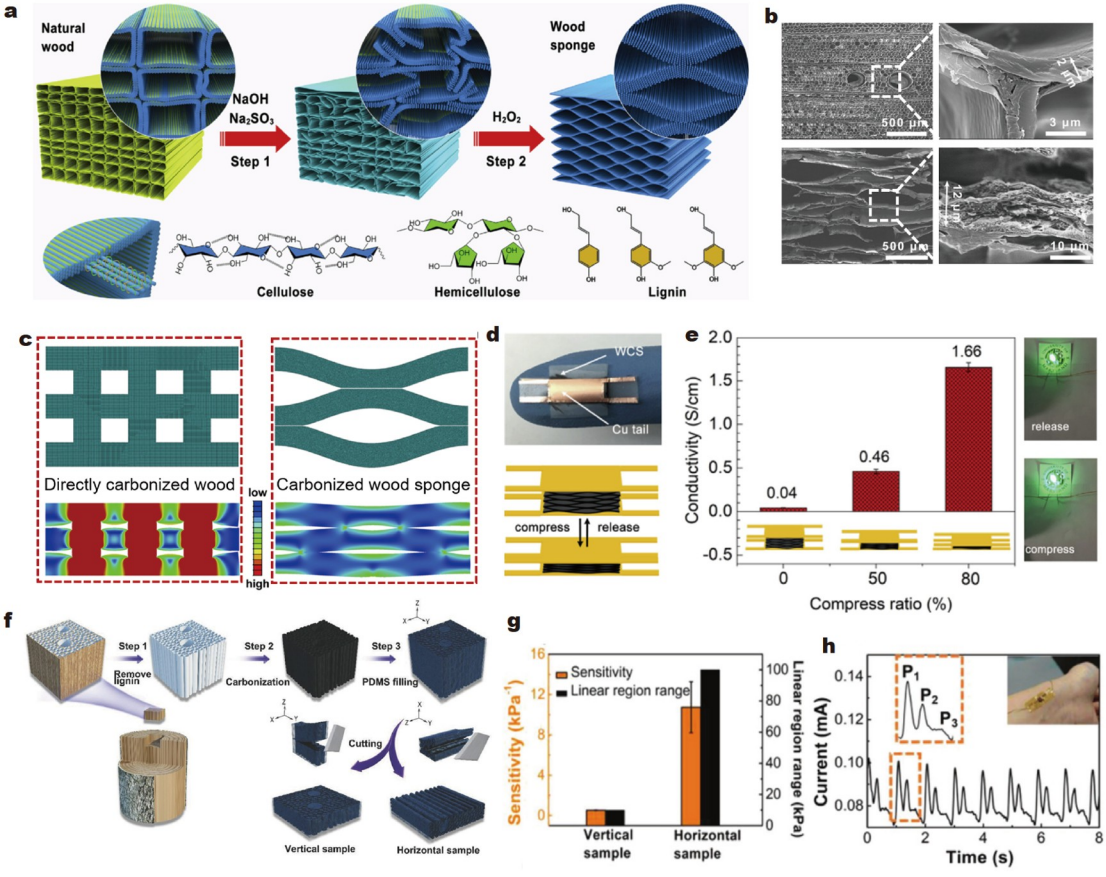

Figure 10 Resistive pressure sensor prepared from wood-derived carbons. (a) Changes in the chemical composition and structure of natural wood during treatment with sodium sulfite, sodium hydroxide and H_2O_2 solution. (b) SEM images of wood before and after treatment with sodium sulfite, sodium hydroxide and H_2O_2. (c) Internal stress distribution of directly carbonized wood and carbonized wood sponges undergoing compressive deformation. (d) Digital photo and working diagram of the carbonized wood sponge pressure sensor. (e) Relationship between the compressive deformation of carbonized wood sponge and electrical conductivity. Reprinted with permission from Ref. [122]. Copyright 2018, Cell Press. (f) Preparation process of the wood sponge/PDMS composite sensor. (g) Pressure sensitivity and linear sensing range of the wood sponge/PDMS composite sensor in different directions. (h) Pulse monitoring behavior of wood sponge/PDMS composite sensors. Reprinted with permission from Ref. [123]. Copyright 2018, Wiley.

nately, this sensor cannot capture subtle movements such as pulse and breath, and this research did not systematically evaluate important parameters such as the sensitivity of the sensors and the sensing range for pressure and strain. To this end, Wong's group [123] washed away most of the lignin and hemicellulose from the wood using a mixture of NaOH and sodium sulfite, and then combined the carbonized wood sponge with PDMS to prepare a composite pressure sensor through a carbonization-permeation strategy (Fig. 10f). The filling of the composite with mechanically stable and resilient PDMS improved the brittle-defect of pure wood sponge, ensuring that the composite sensor recovered to its original state when the mechanical stress was removed [123]. The sensing test results exhibited that the pressure sensitivity and linear sensing range of the wood sponge/PDMS composite sensor could reach 10.74 kPa^{-1} and 100 kPa, respectively (Fig. 10g). Moreover, due to the introduction of highly elastic PDMS, the wood sponge/PDMS composite sensor could even withstand more than 12,000 compression-recovery cycles while maintaining a stable and accurate electrical signal output, demonstrating the sensor's satisfactory fatigue resistance and cycling stability. In addition, when the sensor was fixed on the surface of the body, it showed good detection performance for human motion signals, including limb movement and pulse, manifesting favorable application potential in wearable situations (Fig. 10h).

Besides the natural 3D structures in wood, artificial design and processing can likewise stack cellulose into sponge-like elastomers with 3D network structures, such as aerogels, completing the transformation from 1D to 3D. For example, Zhuo *et al.* [124] chose konjac glucomannan (KGM) as a binder to construct elastic KGM/cellulose nanocrystal (CNC) hybrid aerogels with a 3D network structure relying on the hydrogen bonding between KGM and CNC, and subsequently prepared KGM/CNC-derived carbon aerogel sensors by a carbonization process (Fig. 11a, b). This aerogel sensor had a pressure sensitivity of 8.83 kPa^{-1} in the pressure range of 0–1000 Pa and could resist

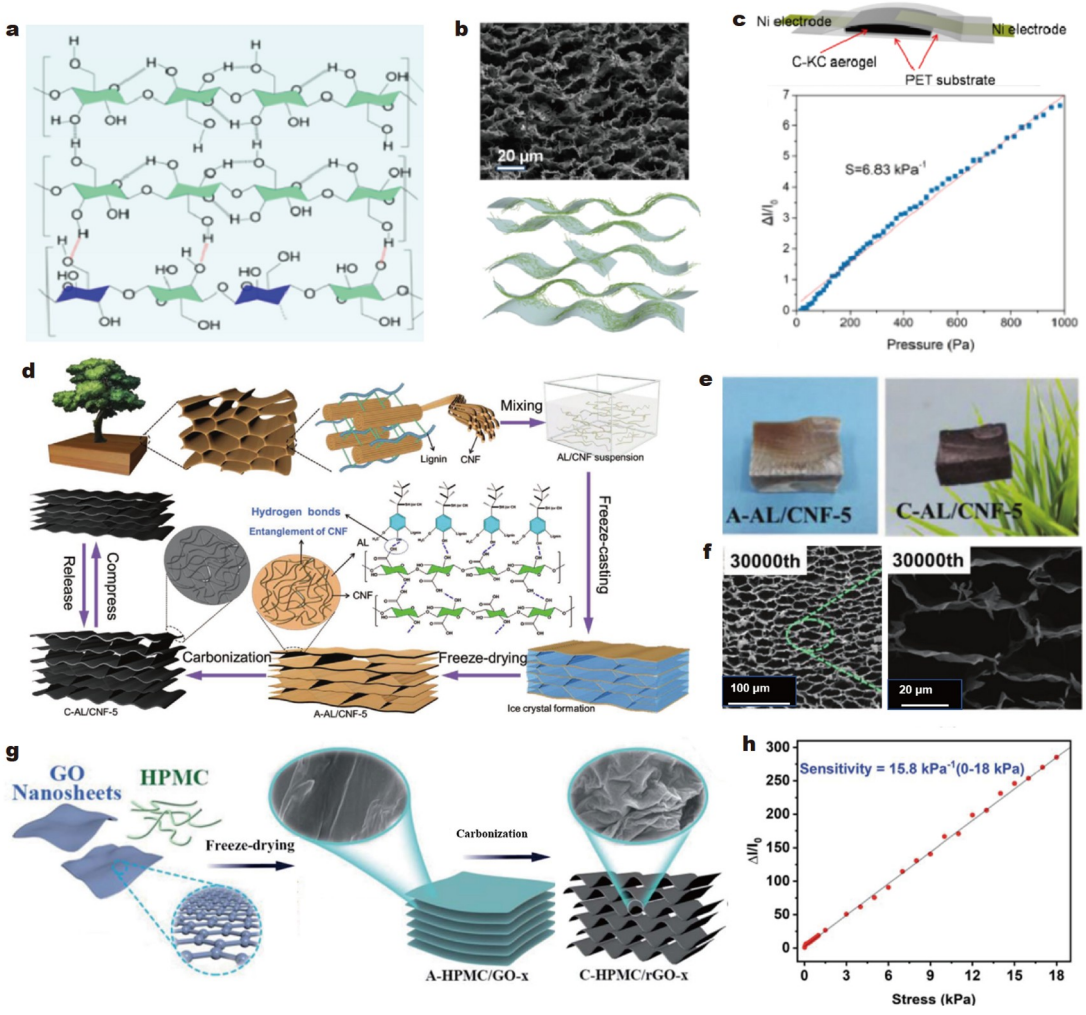

Figure 11 3D resistive pressure sensors based on biomass aerogel-derived carbons. (a) Hydrogen bonding between KGM and CNC molecules. (b) SEM image and structural model of KGM/CNC-derived carbon aerogels. (c) Pressure sensing test of KGM/CNC-derived carbon aerogel-based sensors. Reprinted with permission from Ref. [124]. Copyright 2020, American Chemical Society. (d) Schematic diagram of the preparation process of lignin/CNF-derived carbon aerogel-based sensors. (e) Digital photographs of lignin/CNF aerogels and lignin/CNF-derived carbon aerogels. (f) Microstructure of lignin/CNF-derived carbon aerogel after 30,000 compression-release cycles. Reprinted with permission from Ref. [125]. Copyright 2020, Wiley. (g) Schematic diagram of the preparation of GO/HPMC-derived carbon aerogel. (h) Pressure sensitivity and linear sensing behavior of GO/HPMC-derived carbon aerogels. Reprinted with permission from Ref. [126]. Copyright 2020, Royal Society of Chemistry.

1000 cycles of 90% high compression deformation (Fig. 11c). In addition, nanocellulose fibers (NCF) with large aspect ratios can easily be made into aerogels by freeze-drying methods relying on the intertwining of fibers. Based on this, Peng's group [125] designed a "bottom-up" approach to prepare lightweight lignin/NCF hybrid-derived carbon aerogels (Fig. 11d, e). The existence of lignin with better thermal stability could well prevent excessive deformation of CNF, thus maintaining the volume of the aerogel and ensuring the integrity of the internal network during carbonization. The perfect pore structure led to an outstanding resistance to mechanical fatigue, which resulted in good compression recovery and a homogeneous 3D network even after 30,000 compression-recovery cycles (Fig. 11f). Importantly, this lignin/NCF-derived carbon-based sensor also showed outstanding linear behavior (R^2 = 0.998) with a pressure sensitivity of 5.16 kPa^{-1} in a wide pressure range of 0–16.8 kPa, demonstrating a strong correlation between pressure and electrical signal changes. Furthermore, the response and recovery times of this pressure sensor were 65 and 52 ms, respectively, which could meet the requirement of recording transient pressure changes such as pulses and pronunciations. In order to further improve the sensitivity and other properties of the sensors, numerous conductive materials, such as graphene and CNTs [50], have been introduced into the aerogel system to build a better conductive network. Typically, Jiang *et al.* [126] reported a conductive graphene oxide/hydroxypropyl methyl cellulose (GO/HPMC) composite-based aerogel by carbonizing the freeze-dried GO/HPMC mixture (Fig. 11g). During the carbonization process, GO was reduced and anchored inside the derived carbon network, avoiding the disruption of the aerogel network at high temperatures and inducing the generation of parallel pore structures at the same time. As a result, this GO/HPMC-derived carbon aerogel could withstand nearly 99% of the ultimate compression deformation without any damage. Besides, the introduction of GO endowed the GO/HPMC-derived carbon aerogel with a linear pressure sensitivity of more than 15 kPa^{-1} and a maximum sensing pressure of 18 kPa (Fig. 11h), which significantly improved the comprehensive performance of HPMC-derived carbon aerogel-based sensors.

In addition, chitosan, an abundant and low-cost biomass material with good solubility and renewable properties [127], is considered as another extremely important precursor for deriving carbon. Hu *et al.* [51] dissolved chitosan in a CNC suspension and subsequently prepared chitosan/CNC-derived carbon aerogels by combining freeze-drying with anaerobic carbonization (Fig. 12a, b). The as-prepared derived carbon aerogels exhibited a distinct wavy laminar structure inside, which usually represented excellent compression fatigue resistance (Fig. 12c, d). The compression test results demonstrated that the chitosan/CNC-derived carbon aerogel remained at about 94% of its original height even after 50,000 cycles of compression-release, implying an almost infinite lifetime and exceeding most similar pressure sensors. Remarkably, the carbon aerogel sensor even displayed an extremely high pressure sensitivity of over 103 kPa^{-1} and an excellent linear sensing range of 0–18 kPa. Moreover, an extremely small pressure of 1.0 Pa and tiny deformation of 0.05% could be captured and recorded by the chitosan/CNC-derived carbon aerogel-based sensor. Further,

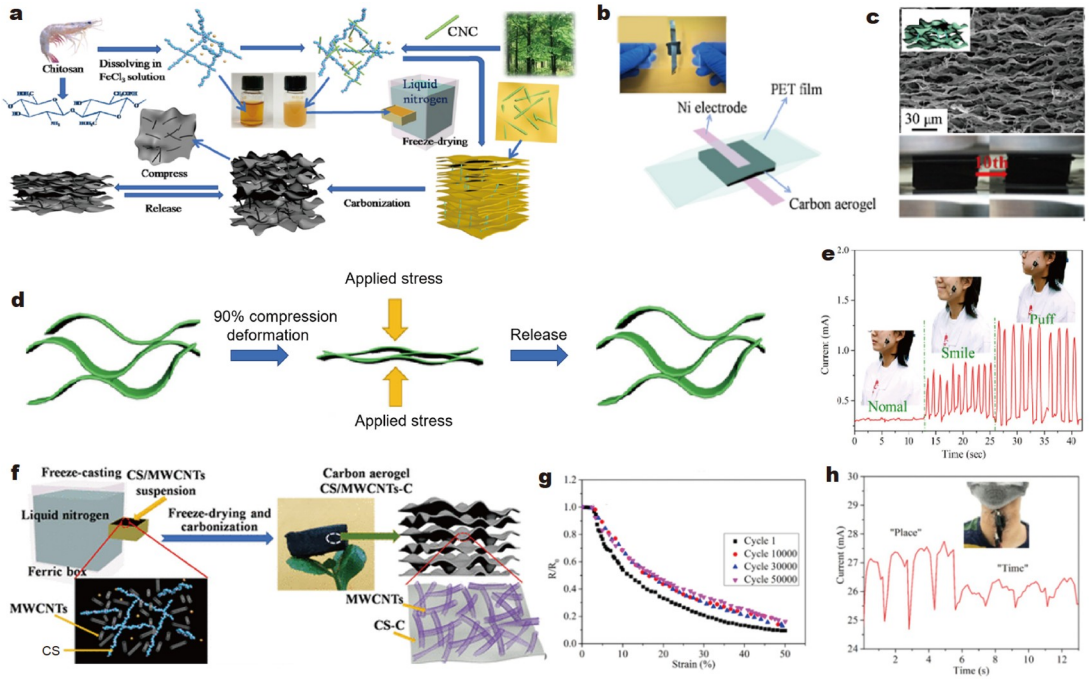

Figure 12 3D resistive pressure sensors based on biomass aerogel-derived carbon. (a) Schematic diagram of the preparation process of chitosan/CNC-derived carbon aerogel. (b) Digital photograph and structural schematic of the chitosan/CNC-derived carbon aerogel-based sensor. (c) Wavy laminar structure and digital photographs of chitosan/CNC-derived carbon aerogels. (d) Schematic diagram of the super-compression and elasticity mechanism of chitosan/CNC-derived carbon aerogel. (e) Sensing behavior of chitosan/CNC-derived carbon aerogel-based sensors for facial movements. Reprinted with permission from Ref. [51]. Copyright 2018, American Chemical Society. (f) Structural schematic of ultralight MWCNT/chitosan-derived carbon aerogel. (g) Relationship between resistance and deformation variables of MWCNT/chitosan-derived carbon aerogel-based sensor at different compression cycles. (h) Detection of human pronunciation by MWCNT/chitosan-derived carbon aerogel-based sensors. Reprinted with permission from Ref. [128]. Copyright 2019, American Chemical Society.

when the chitosan/CNC-derived carbon aerogel-based sensor was attached to the face, it could even sense facial movements such as smiling and puffing (Fig. 12e). Similarly, Zhong's group [128] constructed a hybrid multi-walled CNT (MWCNT)/chitosan-derived carbon aerogel for evaluating compressive sensing performance (Fig. 12f). Chitosan with good adhesion could connect MWCNT into a complete sheet and further form a stable 3D conductive network. This special continuous 3D structure contributed to the outstanding fatigue resistance of the MWCNT/chitosan-derived carbon aerogel and guaranteed compression resistance of more than 50,000 cycles (Fig. 12g). When fixed on the surface of human skin, the carbon aerogel-based sensor could sense pressure stimuli generated by body actions such as limb movements, pronunciation, and facial activity (Fig. 12h). In short, 3D BDC-based sensors, with excellent fatigue resistance along with a perfect 3D network structure, and the ability to accurately monitor different pressures, demonstrate promising application prospects. However, the 3D structure inevitably leads to a larger sensor size, resulting in the difficulty of integration with clothing or wearable devices.

CONCLUSION AND OUTLOOK

Resistive strain/pressure sensors play an irreplaceable role in many applications, including healthcare, motion detection and robotic sensing, and are beginning to have an increasingly profound impact on human life. The trend towards greater refinement, intelligence and environmental friendliness in these applications places higher demands on the materials, structures and performance of resistive strain/pressure sensors. This review summarizes the recent advances in resistive strain/pressure sensors with BDCs as the main conducting network by selecting material type as a unique entry point, systematically describes the sensing mechanism in addition to important performance parameters, and analyzes the construction strategies and advantageous application of BDC-based strain/pressure sensors with different macroscopic structures. So far, BDCs with 1D, 2D and 3D structures have been widely used in resistive strain/pressure sensors, and these sensors have already shown high sensitivity, good sensing stability and ideal monitoring behavior in human motion and health perception. Despite the great achievements, there are still some challenging issues that need to be further overcome for future practical applications (Fig. 13).

First, the preparation conditions of the reported BDCs, such as carbonized cotton, carbonized silk, and carbonized wood aerogel, are harsh, complex, and energy-intensive, which limits the fabrication of high-performance BDC-based sensors to laboratory scale. In practice, it is crucial to develop low-cost, large-scale BDC production technologies to meet the large-scale, standardized manufacture of sensor devices. In addition, even for the same biomass material, there are differences in elemental and molecular structures. For example, the tree variety affects the cellulose and lignin content in the wood, which leads to the differences in the electrical conductivity and mechanical properties of the derived carbon materials. Therefore, new strategies should be explored to eliminate the structural differences of different BDCs and to ensure uniform and stable sensor performance. Importantly, the strain sensing capability of resistive strain/pressure sensors depends on the rates of change in resistance caused by changes in the internal conductive network rather than the resistance value itself, which means that ultra-high conductivity is not a necessary prerequisite for the derived carbon used to prepare the sensors. Therefore, the energy consumption can be reduced in the production process of BDCs by appropriately lowering the carbonization temperature while ensuring the conductive network. In addition, some new techniques can be tried and applied in the preparation of sensors. The use of laser cutting to achieve fine shape control of BDCs, for example, allows for miniaturized sensor design and facilitates the use of devices in narrow spaces. Moreover, 3D printing technology can help transform materials from 1D to 3D, and achieve the unification of macroscopic and microscopic structures of different materials. Some natural polymer hydrogels can be reshaped by 3D printing technology, and may create sensor materials with amazing structures and properties.

Secondly, the high integration of sensors, energy supply devices and test equipment are important and necessary. Currently, the collection and transmission of BDC-based strain/pressure sensor signals rely heavily on external test and analysis instruments, which has gradually become a bottleneck in the real-time recording of human activity or health signals. Therefore, the preparation and measurement of sensors need to focus on the miniaturization and integration to develop flexible and lightweight BDC-based sensing devices for independent monitoring of human signals. For instance, the combination of micro energy storage devices and sensors to achieve the construction of flexible wearable monitoring systems is considered as a promising route [129,130]. This requires consideration regarding compatibility of material systems and preparation technology methods. For example, BDCs can be used as both energy storage and sensing units, so that the simultaneous preparation and

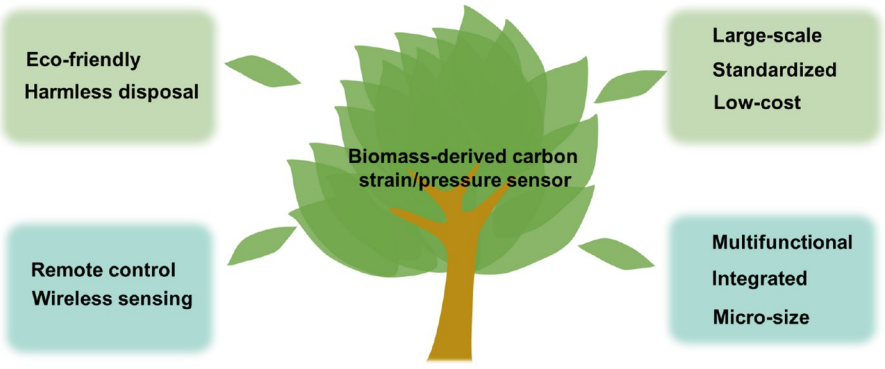

Figure 13 Summary of the future development directions of BDC-based strain/pressure sensors.

performance unification of energy storage and sensor devices can be achieved. Furthermore, the remote controllability and remote monitoring of sensors are the main directions for their development in the future. Therefore, the way to combine the sensors prepared by BDCs with remote control system to realize truly wireless signal transmission is also a problem that needs a solution at present.

Last but not the least, the degradability and non-hazardous disposal of the sensors should also be considered. Despite the good environmental friendliness of BDCs, the large amount of metallic materials and non-degradable substrates in the sensors may cause irreversible pollution and damage to the environment. Therefore, new degradable elastomeric substrate materials need to be designed and prepared to achieve overall environmental friendliness of the sensors and to reduce e-waste. Moreover, the interfacial compatibility between BDCs and the new degradable substrate needs more attention to ensure the stability of the electrical signal transmission during the long-term use of the sensor.

Although impressive progress has been made in the preparation and design of BDC-based strain or pressure sensors, there are still drawbacks such as complex preparation processes, difficulty in integration, and lack of practicality. In this case, unremitting efforts are still required to develop BDC-based strain or pressure sensors for flexible, wearable and even human-machine interaction devices. In addition, with the development of implantable medical treatment, some BDCs with good biocompatibility should be explored and investigated in the field of implantable sensing devices. Human-machine intelligent interaction, as an important development direction for science and technology, will be the most important breakthrough in the application of BDC-based sensors in the future, which requires more attention through interdisciplinary approaches. In summary, with the progress of technology, we believe that the preparation process and design strategy of BDC-based sensors will be dramatically improved and enhanced, and will make an important contribution to the efficient monitoring of human health and finally, usher in the much-awaited "smart future".

Received 11 November 2022; accepted 10 January 2023; published online 14 April 2023

1 Ha M, Lim S, Ko H. Wearable and flexible sensors for user-interactive health-monitoring devices. J Mater Chem B, 2018, 6: 4043–4064
2 Wang X, Liu Z, Zhang T. Flexible sensing electronics for wearable/attachable health monitoring. Small, 2017, 13: 1602790
3 Kim H, Ahn JH. Graphene for flexible and wearable device applications. Carbon, 2017, 120: 244–257
4 Ma C, Ma MG, Si C, *et al.* Flexible MXene-based composites for wearable devices. Adv Funct Mater, 2021, 31: 2009524
5 Wang H, Li Z, Liu Z, *et al.* Flexible capacitive pressure sensors for wearable electronics. J Mater Chem C, 2022, 10: 1594–1605
6 Chao M, Wang Y, Ma D, *et al.* Wearable MXene nanocomposites-based strain sensor with tile-like stacked hierarchical microstructure for broad-range ultrasensitive sensing. Nano Energy, 2020, 78: 105187
7 Liu L, Wang L, Liu X, *et al.* High-performance wearable strain sensor based on MXene@cotton fabric with network structure. Nanomaterials, 2021, 11: 889
8 Huang L, Wang H, Wu P, *et al.* Wearable flexible strain sensor based on three-dimensional wavy laser-induced graphene and silicone rubber. Sensors, 2020, 20: 4266
9 Zhang D, Zhang J, Wu Y, *et al.* Liquid metal interdigitated capacitive strain sensor with normal stress insensitivity. Adv Intelligent Syst, 2022, 4: 2100201
10 Yoon SG, Koo HJ, Chang ST. Highly stretchable and transparent microfluidic strain sensors for monitoring human body motions. ACS Appl Mater Interfaces, 2015, 7: 27562–27570
11 Yang G, Tang X, Zhao G, *et al.* Highly sensitive, direction-aware, and transparent strain sensor based on oriented electrospun nanofibers for wearable electronic applications. Chem Eng J, 2022, 435: 135004
12 Zhang S, Wen L, Wang H, *et al.* Vertical CNT-ecoflex nanofins for highly linear broad-range-detection wearable strain sensors. J Mater Chem C, 2018, 6: 5132–5139
13 Li Z, Ye L, Shen J, *et al.* Strain-gauge sensoring composite films with self-restoring water-repellent properties for monitoring human movements. Compos Commun, 2018, 7: 23–29
14 Lee H, Glasper MJ, Li X, *et al.* Preparation of fabric strain sensor based on graphene for human motion monitoring. J Mater Sci, 2018, 53: 9026–9033
15 Duan S, Wang Z, Zhang L, *et al.* A highly stretchable, sensitive, and transparent strain sensor based on binary hybrid network consisting of hierarchical multiscale metal nanowires. Adv Mater Technol, 2018, 3: 1800020
16 Yin R, Yang S, Li Q, *et al.* Flexible conductive Ag nanowire/cellulose nanofibril hybrid nanopaper for strain and temperature sensing applications. Sci Bull, 2020, 65: 899–908
17 Pan J, Yang M, Luo L, *et al.* Stretchable and highly sensitive braided composite yarn@polydopamine@polypyrrole for wearable applications. ACS Appl Mater Interfaces, 2019, 11: 7338–7348
18 Veeralingam S, Badhulika S. Bi_2S_3/PVDF/PPy-based freestanding, wearable, transient nanomembrane for ultrasensitive pressure, strain, and temperature sensing. ACS Appl Bio Mater, 2021, 4: 14–23
19 Yan T, Wang Z, Pan ZJ. Flexible strain sensors fabricated using carbon-based nanomaterials: A review. Curr Opin Solid State Mater Sci, 2018, 22: 213–228
20 Li S, Xiao X, Hu J, *et al.* Recent advances of carbon-based flexible strain sensors in physiological signal monitoring. ACS Appl Electron Mater, 2020, 2: 2282–2300
21 Jian M, Wang C, Wang Q, *et al.* Advanced carbon materials for flexible and wearable sensors. Sci China Mater, 2017, 60: 1026–1062
22 Li W, Chen Z, Yu H, *et al.* Wood-derived carbon materials and light-emitting materials. Adv Mater, 2021, 33: 2000596
23 Chen L, Bai L, Yeo J, *et al.* Wood-derived carbon with selectively introduced C=O groups toward stable and high capacity anodes for sodium storage. ACS Appl Mater Interfaces, 2020, 12: 27499–27507
24 Deng L, Guo S, Zhou M, *et al.* A silk derived carbon fiber mat modified with Au@Pt urchilike nanoparticles: A new platform as electrochemical microbial biosensor. Biosens Bioelectron, 2010, 25: 2189–2193
25 Matsagar BM, Yang RX, Dutta S, *et al.* Recent progress in the development of biomass-derived nitrogen-doped porous carbon. J Mater Chem A, 2021, 9: 3703–3728
26 Zhu X, Yu S, Xu K, *et al.* Sustainable activated carbons from dead ginkgo leaves for supercapacitor electrode active materials. Chem Eng Sci, 2018, 181: 36–45
27 Deng L, Yuan Y, Zhang Y, *et al. Alfalfa* leaf-derived porous heteroatom-doped carbon materials as efficient cathodic catalysts in microbial fuel cells. ACS Sustain Chem Eng, 2017, 5: 9766–9773
28 Jiang L, Sheng L, Fan Z. Biomass-derived carbon materials with structural diversities and their applications in energy storage. Sci China Mater, 2018, 61: 133–158
29 Chen Y, Guo X, Liu A, *et al.* Recent progress in biomass-derived carbon materials used for secondary batteries. Sustain Energy Fuels, 2021, 5: 3017–3038
30 Wei L, Li JH, Chen C, *et al.* Ultrasensitive non-enzymatic glucose sensors based on hybrid reduced graphene oxide and carbonized silk fabric electrodes decorated with Cu nanoflowers. J Electrochem Soc, 2020, 167: 127501
31 Wu R, Ma L, Patil A, *et al.* Graphene decorated carbonized cellulose fabric for physiological signal monitoring and energy harvesting. J Mater Chem A, 2020, 8: 12665–12673
32 Joshi A, Raulo A, Bandyopadhyay S, *et al.* Waste cotton cloth derived flexible current collector with optimized electrical properties for high

performance lithium-sulfur batteries. Carbon, 2022, 192: 429–437
33 Xu M, Li F, Zhang Z, *et al.* Stretchable and multifunctional strain sensors based on 3D graphene foams for active and adaptive tactile imaging. Sci China Mater, 2019, 62: 555–565
34 Wang C, Hou X, Cui M, *et al.* An ultra-sensitive and wide measuring range pressure sensor with paper-based CNT film/interdigitated structure. Sci China Mater, 2020, 63: 403–412
35 Yang Z, Zhou S, Zu J, *et al.* High-performance piezoelectric energy harvesters and their applications. Joule, 2018, 2: 642–697
36 Fiorillo AS, Critello CD, Pullano SA. Theory, technology and applications of piezoresistive sensors: A review. Sens Actuat A-Phys, 2018, 281: 156–175
37 Miao W, Wang D, Liu Z, *et al.* Bioinspired self-healing liquid films for ultradurable electronics. ACS Nano, 2019, 13: 3225–3231
38 Wu Y, Zhen R, Liu H, *et al.* Liquid metal fiber composed of a tubular channel as a high-performance strain sensor. J Mater Chem C, 2017, 5: 12483–12491
39 Wang Y, Hao J, Huang Z, *et al.* Flexible electrically resistive-type strain sensors based on reduced graphene oxide-decorated electrospun polymer fibrous mats for human motion monitoring. Carbon, 2018, 126: 360–371
40 Huang T, He P, Wang R, *et al.* Porous fibers composed of polymer nanoball decorated graphene for wearable and highly sensitive strain sensors. Adv Funct Mater, 2019, 29: 1903732
41 Liu X, Miao J, Fan Q, *et al.* Recent progress on smart fiber and textile based wearable strain sensors: Materials, fabrications and applications. Adv Fiber Mater, 2022, 4: 361–389
42 Chen W, Yan X. Progress in achieving high-performance piezoresistive and capacitive flexible pressure sensors: A review. J Mater Sci Tech, 2020, 43: 175–188
43 Jin T, Ko Park SH, Fang DW. Highly-stable flexible pressure sensor using piezoelectric polymer film on metal oxide TFT. RSC Adv, 2022, 12: 21014–21021
44 Wang G, Li Y, Cui H, *et al.* Acceleration self-compensation mechanism and experimental research on shock wave piezoelectric pressure sensor. Mech Syst Signal Proc, 2021, 150: 107303
45 Chang S, Li J, He Y, *et al.* A high-sensitivity and low-hysteresis flexible pressure sensor based on carbonized cotton fabric. Sens Actuat A-Phys, 2019, 294: 45–53
46 Zhang L, Li H, Lai X, *et al.* Carbonized cotton fabric-based multilayer piezoresistive pressure sensors. Cellulose, 2019, 26: 5001–5014
47 Tang B, Chen X, He Y, *et al.* Fabrication of kapok fibers and natural rubber composites for pressure sensor applications. Cellulose, 2021, 28: 2287–2301
48 Lu W, Yu P, Jian M, *et al.* Molybdenum disulfide nanosheets aligned vertically on carbonized silk fabric as smart textile for wearable pressure-sensing and energy devices. ACS Appl Mater Interfaces, 2020, 12: 11825–11832
49 Wang Q, Jian M, Wang C, *et al.* Carbonized silk nanofiber membrane for transparent and sensitive electronic skin. Adv Funct Mater, 2017, 27: 1605657
50 Liu H, Xu T, Cai C, *et al.* Multifunctional superelastic, superhydrophilic, and ultralight nanocellulose-based composite carbon aerogels for compressive supercapacitor and strain sensor. Adv Funct Mater, 2022, 32: 2113082
51 Hu Y, Zhuo H, Chen Z, *et al.* Superelastic carbon aerogel with ultrahigh and wide-range linear sensitivity. ACS Appl Mater Interfaces, 2018, 10: 40641–40650
52 He X, Shen G, Liang J, *et al.* Stretchable strain sensors based on two- and three-dimensional carbonized cotton fabrics for the detection of full range of human motions. ACS Appl Electron Mater, 2021, 3: 3287–3295
53 Wang C, Xia K, Jian M, *et al.* Carbonized silk georgette as an ultrasensitive wearable strain sensor for full-range human activity monitoring. J Mater Chem C, 2017, 5: 7604–7611
54 Xia K, Chen X, Shen X, *et al.* Carbonized Chinese art paper-based high-performance wearable strain sensor for human activity monitoring. ACS Appl Electron Mater, 2019, 1: 2415–2421
55 Ji T, Sun H, Cui B, *et al.* Sustainable and conductive wood-derived carbon framework for stretchable strain sensors. Adv Sustain Syst, 2022, 6: 2100382
56 Zhang M, Wang C, Wang H, *et al.* Carbonized cotton fabric for high-performance wearable strain sensors. Adv Funct Mater, 2017, 27: 1604795
57 Zhu WB, Li YQ, Wang J, *et al.* High-performance fiber-film hybrid-structured wearable strain sensor from a highly robust and conductive carbonized bamboo aerogel. ACS Appl Bio Mater, 2020, 3: 8748–8756
58 Chen S, Song Y, Ding D, *et al.* Flexible and anisotropic strain sensor based on carbonized crepe paper with aligned cellulose fibers. Adv Funct Mater, 2018, 28: 1802547
59 Gao Y, Xiao T, Li Q, *et al.* Flexible microstructured pressure sensors: Design, fabrication and applications. Nanotechnology, 2022, 33: 322002
60 Wang X, Chai Y, Wang Z, *et al.* Metal oxides/carbon felt pressure sensors with ultra-broad-range high sensitivity. Adv Mater Inter, 2022, 9: 2101663
61 Li C, Pan L, Deng C, *et al.* A highly sensitive and wide-range pressure sensor based on a carbon nanocoil network fabricated by an electrophoretic method. J Mater Chem C, 2017, 5: 11892–11900
62 Hosseini ES, Chakraborty M, Roe J, *et al.* Porous elastomer based wide range flexible pressure sensor for autonomous underwater vehicles. IEEE Sens J, 2022, 22: 9914–9921
63 Han W, Wu Y, Gong H, *et al.* Reliable sensors based on graphene textile with negative resistance variation in three dimensions. Nano Res, 2021, 14: 2810–2818
64 Wu L, Xu C, Fan M, *et al.* Lotus root structure-inspired Ti_3C_2-MXene-based flexible and wearable strain sensor with ultra-high sensitivity and wide sensing range. Compos Part A-Appl Sci Manufact, 2022, 152: 106702
65 Wu L, Fan M, Qu M, *et al.* Self-healing and anti-freezing graphene-hydrogel-graphene sandwich strain sensor with ultrahigh sensitivity. J Mater Chem B, 2021, 9: 3088–3096
66 Yue Z, Zhu Y, Xia J, *et al.* Sponge graphene aerogel pressure sensors with an extremely wide operation range for human recognition and motion detection. ACS Appl Electron Mater, 2021, 3: 1301–1310
67 Wei H, Kong D, Li T, *et al.* Solution-processable conductive composite hydrogels with multiple synergetic networks toward wearable pressure/strain sensors. ACS Sens, 2021, 6: 2938–2951
68 Souri H, Banerjee H, Jusufi A, *et al.* Wearable and stretchable strain sensors: Materials, sensing mechanisms, and applications. Adv Intelligent Syst, 2020, 2: 2000039
69 Fan M, Wu L, Hu Y, *et al.* A highly stretchable natural rubber/buckypaper/natural rubber (NR/N-BP/NR) sandwich strain sensor with ultrahigh sensitivity. Adv Compos Hybrid Mater, 2021, 4: 1039–1047
70 Paul SJ, Elizabeth I, Gupta BK. Ultrasensitive wearable strain sensors based on a VACNT/PDMS thin film for a wide range of human motion monitoring. ACS Appl Mater Interfaces, 2021, 13: 8871–8879
71 Wu L, Li L, Qu M, *et al.* Mussel-inspired self-adhesive, antidrying, and antifreezing poly(acrylic acid)/bentonite/polydopamine hybrid glycerol-hydrogel and the sensing application. ACS Appl Polym Mater, 2020, 2: 3094–3106
72 Tang N, Zhou C, Qu D, *et al.* A highly aligned nanowire-based strain sensor for ultrasensitive monitoring of subtle human motion. Small, 2020, 16: 2001363
73 Huang J, Zhou J, Luo Y, *et al.* Wrinkle-enabled highly stretchable strain sensors for wide-range health monitoring with a big data cloud platform. ACS Appl Mater Interfaces, 2020, 12: 43009–43017
74 Liu X, Miao J, Fan Q, *et al.* Recent progress on smart fiber and textile based wearable strain sensors: Materials, fabrications and applications. Adv Fiber Mater, 2022, 4: 571
75 Lei H, Dong L, Li Y, *et al.* Stretchable hydrogels with low hysteresis and anti-fatigue fracture based on polyprotein cross-linkers. Nat Commun, 2020, 11: 4032
76 Wang Y, Pang B, Wang R, *et al.* An anti-freezing wearable strain sensor based on nanoarchitectonics with a highly stretchable, tough, anti-fatigue and fast self-healing composite hydrogel. Compos Part A-Appl Sci Manufact, 2022, 160: 107039

77 Lu J, Hu O, Gu J, *et al.* Tough and anti-fatigue double network gelatin/polyacrylamide/DMSO/Na_2SO_4 ionic conductive organohydrogel for flexible strain sensor. Eur Polym J, 2022, 168: 111099
78 Li T, Zhi DD, Guo ZH, *et al.* 3D porous biomass-derived carbon materials: Biomass sources, controllable transformation and microwave absorption application. Green Chem, 2022, 24: 647–674
79 Jin C, Nai J, Sheng O, *et al.* Biomass-based materials for green lithium secondary batteries. Energy Environ Sci, 2021, 14: 1326–1379
80 Yang Z, Chaieb S, Hemar Y. Gelatin-based nanocomposites: A review. Polym Rev, 2021, 61: 765–813
81 Qu B, Luo Y. Chitosan-based hydrogel beads: Preparations, modifications and applications in food and agriculture sectors—A review. Int J Biol Macromolecules, 2020, 152: 437–448
82 Liu WJ, Jiang H, Yu HQ. Thermochemical conversion of lignin to functional materials: A review and future directions. Green Chem, 2015, 17: 4888–4907
83 Wang X, Yao C, Wang F, *et al.* Cellulose-based nanomaterials for energy applications. Small, 2018, 14: 1704152
84 Ummartyotin S, Manuspiya H. A critical review on cellulose: From fundamental to an approach on sensor technology. Renew Sustain Energy Rev, 2015, 41: 402–412
85 Chio C, Sain M, Qin W. Lignin utilization: A review of lignin depolymerization from various aspects. Renew Sustain Energy Rev, 2019, 107: 232–249
86 Agustin MB, Carvalho DM, Lahtinen MH, *et al.* Laccase as a tool in building advanced lignin-based materials. ChemSusChem, 2021, 14: 4615–4635
87 Deng J, Xiong T, Wang H, *et al.* Effects of cellulose, hemicellulose, and lignin on the structure and morphology of porous carbons. ACS Sustain Chem Eng, 2016, 4: 3750–3756
88 Duan B, Huang Y, Lu A, *et al.* Recent advances in chitin based materials constructed *via* physical methods. Prog Polym Sci, 2018, 82: 1–33
89 Bartlett DH, Azam F. Chitin, cholera, and competence. Science, 2005, 310: 1775–1777
90 Nogi M, Kurosaki F, Yano H, *et al.* Preparation of nanofibrillar carbon from chitin nanofibers. Carbohydrate Polyms, 2010, 81: 919–924
91 Wang Y, Zhang M, Shen X, *et al.* Biomass-derived carbon materials: Controllable preparation and versatile applications. Small, 2021, 17: 2008079
92 Li YQ, Samad YA, Polychronopoulou K, *et al.* Lightweight and highly conductive aerogel-like carbon from sugarcane with superior mechanical and EMI shielding properties. ACS Sustain Chem Eng, 2015, 3: 1419–1427
93 Qiao Y, Chen S, Liu Y, *et al.* Pyrolysis of chitin biomass: TG-MS analysis and solid char residue characterization. Carbohydrate Polyms, 2015, 133: 163–170
94 Hu M, Hu T, Cheng R, *et al.* MXene-coated silk-derived carbon cloth toward flexible electrode for supercapacitor application. J Energy Chem, 2018, 27: 161–166
95 He W, Wang C, Wang H, *et al.* Integrated textile sensor patch for real-time and multiplex sweat analysis. Sci Adv, 2019, 5: eaax0649
96 Sugimoto Y, Irisawa T, Hatori H, *et al.* Yarns of carbon nanotubes and reduced graphene oxides. Carbon, 2020, 165: 358–377
97 Jang Y, Kim SM, Spinks GM, *et al.* Carbon nanotube yarn for fiber-shaped electrical sensors, actuators, and energy storage for smart systems. Adv Mater, 2020, 32: 1902670
98 Liu F, Dong Y, Shi R, *et al.* Continuous graphene fibers prepared by liquid crystal spinning as strain sensors for monitoring vital signs. Mater Today Commun, 2020, 24: 100909
99 Yan T, Wang Z, Wang YQ, *et al.* Carbon/graphene composite nanofiber yarns for highly sensitive strain sensors. Mater Des, 2018, 143: 214–223
100 Tang J, Wu Y, Ma S, *et al.* Flexible strain sensor based on CNT/TPU composite nanofiber yarn for smart sports bandage. Compos Part B-Eng, 2022, 232: 109605
101 Shang Y, Li Y, He X, *et al.* Elastic carbon nanotube straight yarns embedded with helical loops. Nanoscale, 2013, 5: 2403–2410
102 Li Y, Shang Y, He X, *et al.* Overtwisted, resolvable carbon nanotube yarn entanglement as strain sensors and rotational actuators. ACS Nano, 2013, 7: 8128–8135
103 Yan T, Wu Y, Tang J, *et al.* Highly sensitive strain sensor with wide strain range fabricated using carbonized natural wrapping yarns. Mater Res Bull, 2021, 143: 111452
104 Das S, Natarajan S. Deformation behaviour of mulberry woven silk fabrics. J Nat Fibers, 2022, 19: 10946–10952
105 Gao D, Li X, Li Y, *et al.* Long-acting antibacterial activity on the cotton fabric. Cellulose, 2021, 28: 1221–1240
106 Wang C, Li X, Gao E, *et al.* Carbonized silk fabric for ultrastretchable, highly sensitive, and wearable strain sensors. Adv Mater, 2016, 28: 6640–6648
107 Zhang J, Long H, Zhang P. Structure and characterization of carbonized cotton knitted fabric. Textile Res J, 2022, 92: 3719–3732
108 Dai X, Guo Z. The gorgeous transformation of paper: From cellulose paper to inorganic paper to 2D paper materials with multifunctional properties. J Mater Chem A, 2021, 10: 122–156
109 Chen S, Song Y, Xu F. Flexible and highly sensitive resistive pressure sensor based on carbonized crepe paper with corrugated structure. ACS Appl Mater Interfaces, 2018, 10: 34646–34654
110 Wang L, Zhang M, Yang B, *et al.* Recent advances in multidimensional (1D, 2D, and 3D) composite sensors derived from MXene: Synthesis, structure, application, and perspective. Small Methods, 2021, 5: 2100409
111 Wang X, Wang X, Yin J, *et al.* Mechanically robust, degradable and conductive MXene-composited gelatin organohydrogel with environmental stability and self-adhesiveness for multifunctional sensor. Compos Part B-Eng, 2022, 241: 110052
112 Lee KH, Zhang Y, Kim H, *et al.* Muscle fatigue sensor based on $Ti_3C_2T_x$ MXene hydrogel. Small Methods, 2021, 5: 2100819
113 Zheng Y, Yin R, Zhao Y, *et al.* Conductive MXene/cotton fabric based pressure sensor with both high sensitivity and wide sensing range for human motion detection and E-skin. Chem Eng J, 2021, 420: 127720
114 Lee J, Kim J, Liu D, *et al.* Highly aligned, anisotropic carbon nanofiber films for multidirectional strain sensors with exceptional selectivity. Adv Funct Mater, 2019, 29: 1901623
115 Zhang L, Song T, Shi L, *et al.* Recent progress for silver nanowires conducting film for flexible electronics. J Nanostruct Chem, 2021, 11: 323–341
116 He J, Guo X, Yu J, *et al.* A high-resolution flexible sensor array based on PZT nanofibers. Nanotechnology, 2020, 31: 155503
117 Guan QF, Han ZM, Yang HB, *et al.* Regenerated isotropic wood. Natl Sci Rev, 2021, 8: nwaa230
118 Li SC, Hu BC, Ding YW, *et al.* Wood-derived ultrathin carbon nanofiber aerogels. Angew Chem Int Ed, 2018, 57: 7085–7090
119 He W, Qiang H, Liang S, *et al.* Hierarchically porous wood aerogel/polypyrrole(PPy) composite thick electrode for supercapacitor. Chem Eng J, 2022, 446: 137331
120 Zhang Q, Li L, Jiang B, *et al.* Flexible and mildew-resistant wood-derived aerogel for stable and efficient solar desalination. ACS Appl Mater Interfaces, 2020, 12: 28179–28187
121 Song J, Chen C, Yang Z, *et al.* Highly compressible, anisotropic aerogel with aligned cellulose nanofibers. ACS Nano, 2018, 12: 140–147
122 Chen C, Song J, Zhu S, *et al.* Scalable and sustainable approach toward highly compressible, anisotropic, lamellar carbon sponge. Chem, 2018, 4: 544–554
123 Huang Y, Chen Y, Fan X, *et al.* Wood derived composites for high sensitivity and wide linear-range pressure sensing. Small, 2018, 14: 1801520
124 Zhuo H, Hu Y, Chen Z, *et al.* Linking renewable cellulose nanocrystal into lightweight and highly elastic carbon aerogel. ACS Sustain Chem Eng, 2020, 8: 11921–11929
125 Chen Z, Zhuo H, Hu Y, *et al.* Wood-derived lightweight and elastic carbon aerogel for pressure sensing and energy storage. Adv Funct Mater, 2020, 30: 1910292
126 Jiang W, Yao C, Chen W, *et al.* A super-resilient and highly sensitive graphene oxide/cellulose-derived carbon aerogel. J Mater Chem A, 2020, 8: 18376–18384

127 Balusamy SR, Rahimi S, Sukweenadhi J, *et al.* Chitosan, chitosan nanoparticles and modified chitosan biomaterials, a potential tool to combat salinity stress in plants. Carbohydrate Polyms, 2022, 284: 119189
128 Luo Q, Zheng H, Hu Y, *et al.* Carbon nanotube/chitosan-based elastic carbon aerogel for pressure sensing. Ind Eng Chem Res, 2019, 58: 17768–17775
129 Zheng S, Ma J, Fang K, *et al.* High-voltage potassium ion micro-supercapacitors with extraordinary volumetric energy density for wearable pressure sensor system. Adv Energy Mater, 2021, 11: 2003835
130 Zheng S, Wang H, Das P, *et al.* Multitasking MXene inks enable high-performance printable microelectrochemical energy storage devices for all-flexible self-powered integrated systems. Adv Mater, 2021, 33: 2005449

Acknowledgements This work was financially supported by the National Natural Science Foundation of China (22125903, 51872283, and 22109160), Dalian Innovation Support Plan for High Level Talents (2019RT09), Dalian National Laboratory For Clean Energy (DNL), CAS, DNL Cooperation Fund, CAS (DNL201912, DNL201915, DNL202016, and DNL202019), DICP (DICP I2020032), the Joint Fund of Yulin University and Dalian National Laboratory for Clean Energy (YLU-DNL Fund 2021002 and YLU-DNL Fund 2021009), and China Postdoctoral Science Foundation (2021M693126).

Author contributions Wu ZS supervised this project. Wu L, Shi X and Wu ZS wrote this manuscript. Das P revised and polished the language. All authors contributed to the general discussion.

Conflict of interest The authors declare that they have no conflict of interest.

Lu Wu is a postdoctoral researcher at Dalian Institute of Chemical Physics, Chinese Academy of Sciences (DICP, CAS). He received his PhD degree from Dalian University of Technology in 2021. His research focuses on the preparation of gel composites and their applications in the field of flexible sensors.

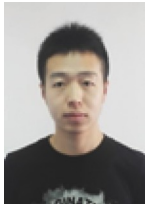

Xiaoyu Shi is a postdoctoral researcher at DICP, CAS. He received his PhD degree from the University of Science and Technology of China in 2020. His research focuses on functional and integrated microscale energy systems.

Pratteek Das is a postdoctoral researcher at DICP, CAS. He received his PhD degree from Dalian Institute of Chemical Physics, CAS in 2022. His research focuses on 2D materials and micro-supercapacitors.

Zhong-Shuai Wu received his PhD degree from the Institute for Metal Research, CAS, in 2011 and worked as a postdoctoral fellow at Max Planck Institute for Polymer Research in Mainz, Germany, from 2011 to 2015. Subsequently, he became a full professor and group leader of 2D Materials Chemistry & Energy Applications at DICP, CAS, and was promoted in 2018 as a DICP Chair Professor. Currently, his research interests include the chemistry of graphene and 2D materials, surface- and nanoelectrochemistry, microscale electrochemical energy storage devices, supercapacitors, batteries, and energy catalysis.

生物质衍生碳在电阻式应变/压力传感器中的最新应用进展与关键挑战

吴鲁[1†], 师晓宇[1†], Pratteek Das[1], 吴忠帅[1,2*]

摘要 近年来电阻式应变/压力传感器在运动行为监测、人类健康诊断和人机交互等领域展现了不可替代的作用，因而刺激了人们对其需求的急剧增长. 材料和结构设计对电阻式应变/压力传感器的性能有着不可忽视的影响，而生物质碳(BDCs)具有丰富的来源、多样的结构和令人满意的导电性等优良特性，被认为是制造电阻式应变/压力传感器的优异候选材料之一. 本综述介绍了BDCs材料在电阻式应变/压力传感器领域的最新进展及其目前面临的主要挑战. 首先，系统地概述和讨论了已报道的电阻式应变/压力传感器的分类方法、评价标准和传感机制. 其次，总结了具有不同宏观结构(包括一维、二维和三维结构)的BDCs材料的制备及其在电阻式应变/压力传感器领域的最新应用进展. 详细分析了具有不同宏观结构的BDCs材料在电阻应变/压力传感器领域的各自应用优势，并讨论了不同宏观结构与器件综合传感性能之间的关系. 最后，提出了基于BDCs材料的电阻式应变/压力传感器的未来前景和主要挑战，及其未来发展的研究方向.

